Optimal techno-economic renewable energy solution assessment of an aquaculture case study
-PEGE I-

Author	Nicolas Soehlemann (ist1113382)
Technical supervisor	Helena M. Ramos (helena.ramos@tecnico.ulisboa.pt)
Management supervisor	Antonio Quintino (antonio.quintino@tecnico.ulisboa.pt)
Semester	S2 2024/2025
Date	19th June 2025

Abstract

Hybrid Renewable Energy Systems score with improved self-sufficiency while reducing the strain on the grid. This project focuses on an aquaculture case study in Ireland which is part of the HY4RES project. The system includes a flexible load, as well as a small hydropower plant and wind turbine. The question arises on how to improve the system economically but also in terms of emission reductions. To validate the simulation approach by the HY4RES model, its performance is compared with the one from HOMER Pro. Then, HY4RES V2, an Excel based techno-economic assessment tool which is tailored to this case study, is developed. An optimization of the different sites as well as sensitivity analysis is conducted with HY4RES V2. The results show good alignment of the two models — HY4RES and HOMER Pro — for grid tied scenarios. HY4RES V2's optimization of the primary site with the Evolutionary method results in a Net Present Value (NPV) of 957.85 € and a payback period of 23.22 years with an 8 kW_p PV system. The sensitivity analysis shows a strong impact by a 10 % increase in PV investment cost, leading to a negative NPV of −396 €. The remaining sensitivity analysis leads to positive NPV values. The secondary site and combined site are well balanced and allow for no optimization. Optimizing the self-sufficiency to 99 % leads to an emission reduction of 77 % for the combined site, but also a negative NPV of −4, 562, 928 €. Using the optimal scenarios, in terms of NPV, it becomes evident that the combined site scores better in terms of emission reduction and higher grid independence while the separate sites are to be preferred economically.

Contents

Glossary

BESS Battery Energy Storage System.

BG Biomass-gasifier ICE.

C&I Commercial & Industrial.

CHP Combined Heat and Power.

DCF Discounted Cash-Flows.

EMS Energy Management System.

EPR Energy-to-Power Ratio.

FCF Free Cash-Flows.

GA Genetic Algorithm.

GPC Gize Pyramids Construction.

GRG Generalized Reduced Gradient.

HRES Hybrid Renewable Energy System.

ICF Investment Cash-Flows.

IRR Internal Rate of Return.

LCOE Levelized Cost of Electricity.

LHV Lower Heating Value.

LP Linear Programming.

MIRR Modified Internal Rate of Return.

NPV Net Present Value.

OCF Operating Cash-Flows.

PP Payback Period.

PPA Power Purchase Agreement.

PSO Particle Swarm Optimization.

PV Photovoltaic.

SCR Self-Consumption Ratio.

SHP Small Hydropower Plant.

SOC State of Health.

SSR Self-Sufficiency Ratio.

WWTP Waste Water Treatment Plant.

1 Introduction

The increasing penetration of distributed energy resource in the power grid can lead to grid congestion [1] and reduced profits for asset owners. Grid operators are wary and connection of newly built assets are queuing for approval [2]. Hybrid Renewable Energy System (HRES) are one solution to this problem [3]. They combine a variety of renewable energy technologies and preferably are located in the near vicinity of a local consumption hub [4]. Due to the complimentary nature of different renewable energy technologies, the self-sufficiency of HRES is higher compared to single resource systems. This helps to alleviate pressure from the power grid and benefits local stakeholders. Among the most common technologies being researched for the integration in HRES are solar Photovoltaic (PV), Battery Energy Storage System (BESS) and wind turbines. Other technologies that appear less frequently include biomass-gasifier ICE units, Small Hydropower Plant (SHP) and hydrogen electrolysers [5].

This project is part of HY4RES, an Interreg Atlantic Area program co-funded by the European Union. Different case studies lie within the HY4RES project frame and were already analyzed in terms of their hybridization potential. Coehlo et al. examine the water-energy nexus for a irrigation site in Spain [6, 7]. The most promising system scenario includes wind turbines, solar PV and utilizes the water reservoir for irrigation also as a pumped hydropower storage plant. By including the wind turbines, grid consumption is reduced by 60 %, making this scenario the most viable economically. H.M. Ramos et al. on the other hand compare different optimization techniques for port's hybrid renewable energy systems and propose energy management strategies based on AI-driven forecasting [8]. In another paper, H.M. Ramos et al. compare different sizes of a HRES with a pumped hydropower storage plant, wind turbines and a PV system. They highlight the importance of sizing each component correctly for a highly efficient system and come to the conclusion that larger HRES systems benefit from their size economically and technologically [9]. The specific goal of HY4RES with its aquaculture case study is to show the potential of hybrid renewable power systems in the decarbonization of the aquaculture sector. Additionally, it will show how to effectively and efficiently balance supply and demand in a complex hybrid energy system, utilizing variable supply and demand patterns to enhance the system's operation. All of this is to be achieved while optimizing the system on cost savings and emission reduction [10]. The system consists of a small hydro power plant, a wind turbine, a waste water treatment facility, a wood drying kiln and two fish processing facilities.

As HRES are complex, due to the combination of renewable energy technologies, different loads and energy storage, optimization of HRES has been the focus of many research papers [5, 11]. For simple economic optimization of HRES, traditional methods such as Linear Programming (LP) or Generalized Reduced Gradient (GRG) are available. For more complex optimization problems with more than one objective function and a large number of decision variables, modern methods such as Evolutionary Strategy or Genetic Algorithm (GA) can be applied [5]. Furthermore, commercial tools such as HOMER Pro offer advantages in setting up the simulation and score with a good user experience, but have their limitations for more specific applications such as the integration of flexible loads. Additionally, its optimization methods are often a black box and only offer simple, single objective function optimization [5]. Due to the complexity and diverse goals of optimization of HRES, models based on Python or Excel are developed and used. However, the accuracy of these models must be confirmed. For this purpose, a comparison with commercial, well-proven software such as HOMER Pro is recommendable [7].

Often, the optimal sizing of the components of an HRES is the main topic of research. However, these studies mostly focus on HRES that are designed from scratch without an existing system [5, 11]. Gusain et al. compare Gize Pyramids Construction (GPC) with Particle Swarm Optimization (PSO) optimization techniques on an HRES based on PV, wind and BESS. They find that the newly proposed GPC method improves the global optimum, leading to a 177 $ decrease in annual cost and reduces simulation time by 8 % [12]. Ukoima et al. on the other hand combine a GA wiht PSO to optimize a PV, BESS and wind HRES. Their results lead to an annual system cost of 297,100 $ and a Levelized Cost of Electricity (LCOE) of 0.007 $\frac{\$}{\mathrm{kWh}}$ [13]. a In order to leverage the full potential of HRES, their integration with existing systems, as well as commercial or community loads should be prioritized.

This research will bridge the research gap outlined above and compare the performance of the existing HY4RES model from Coelho et al. [6] with the one of HOMER Pro. In a next steps the lessons learned are applied to the creation of a more suitable Excel model for the aquaculture case study — HY4RES V2. In the second part, Evolutionary and GRG methods are used in Excel's Solver for optimally sizing the extension of the H4YRES aquaculture case study in Ireland. Combining the existing wind turbine and hydropower plant with solar PV, a biomass-gasifier ICE unit and BESS will highlight the most suitable technology combinations and their optimal size. A thorough techno-economic assessment is conducted and the uncertainties of the crucial input parameters highlighted in a sensitivity analysis. Finally, the optimal scenarios for the site are compared. This report starts with section 2 by presenting the methods used for the comparison between HOMER Pro and HY4RES and the ones for the newly developed model HY4RES V2. Additionally, the input parameters and assumptions are highlighted in section 2. Next, the results from the comparison and HY4RES V2 are presented in section 3. It is followed by a thorough discussion of the results in section 4. Finally, a conclusion of the work is given in combination with recommendations for future research in section 5.

2 Methods

2.1 Aquaculture case study

The case study observed for this project is located in the North-West of Ireland in the Donegal County [10]. It comprises of two aquaculture companies, Island Seafoods and Albatross Seafoods, each producing different value-added fish and seafoods products. The water from the two processing facilities is treated in a Waste Water Treatment Plant (WWTP) on-site. On the generation side a wind turbine and a SHP are installed. Recently, it was decided to install a biomass drying kiln next to the wind turbine to utilize excess electricity that can't be fed into the grid due to a power limitation for grid injection. In reality the primary and secondary site are separate systems, each connected individually to the power grid, due to regulatory restrictions. This is depicted in Figure 1. The depiction is only of symbolic nature, for a more accurate representation of the real site, the reader is invited to visit the interactive video on the HY4RES website [10]. To analyze the viability of extending the system with other renewable energy technologies and storage, the system is considered as one for this project. Hence, utilizing the SHP and wind generation to meet the demand of the loads.

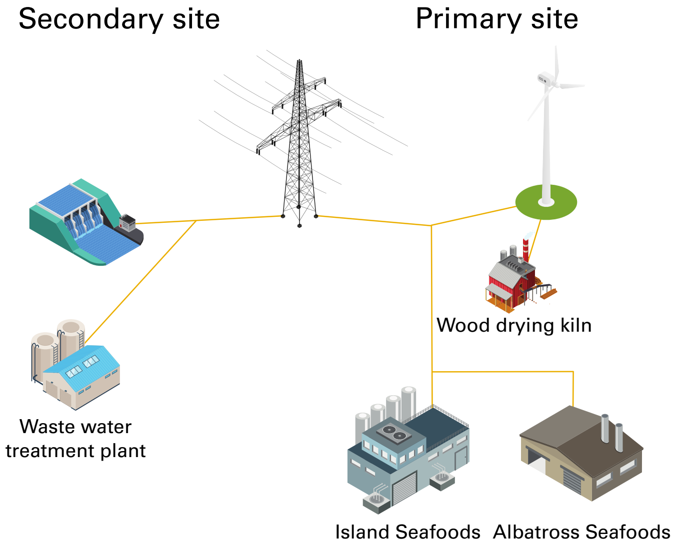

Figure 1: Aquaculture case study, subdivided into the primary and secondary site. With icons designed by macrovector_official and published on FREEPIK.

Island Seafoods has collected 10 years of electricity generation and consumption data which is available for this project. This includes consumption data of the WWTP and generation data for the SHP plant.

2.2 HY4RES model

The HY4RES model was originally designed by Coelho et al. for the water-energy nexus [6]. Two models were created, one more sophisticated based on Python for multi-objective optimization and the other in Excel for single-objective optimization. In this work, the focus lies on the latter, as such the Excel model is referred to HY4RES model from now on. It is designed to optimize the contribution of different renewable energy technologies to the energy demand for pumping water into a reservoir which is used for irrigation purposes while also acting as a pumped hydro storage system. Hence, irrigation demand as well as energy demand of the system must be met. The Evolutionary method is used as the optimization technique in Excel's Solver. The simulation itself has a range of input parameters. Among them are the hourly water and electricity needs, the hourly grid purchase and feed-in prices and the hourly generation data for wind, PV and one more generation technology of choice. Additionally, the specifications of each technology are defined , including reservoir data, hydropower parameters and those of the BESS. The model is designed to either operate grid connected or off-grid with a BESS. Once all the input data are set, the model simulates the energy balance, considering hourly loads and generation. Excess electricity can be used to pump water into the reservoir or feed into the grid. At the end the grid cash-flow is computed and several graphs with the hourly profiles depicted as an output. The tool does not include an in-depth financial analysis, it only takes grid cash-flows into account.

As this case study does not include water needs, the HY4RES model has to be adapted and can be simplified. The model's result are compared later with those from HOMER Pro. Hence, the adaptation of the HY4RES model is primarily to enable a viable comparison between the tools, taking this aquaculture case study into account. As a first step, the water needs are set to 0 and all the pump variables as well. This deactivates the hydropower generation from the reservoir. Furthermore, the computation of the energy excess/deficit is adjusted to enable grid and BESS operation simultaneously. Several renewable technologies are integrated in this case study. Therefore, one more alternative energy generation technology is added in the input sheet and in the simulation itself. Hydropower on the other hand is inserted with a separate hourly generation profile, instead of it relying on the reservoir. Finally, another sheet is added in the Excel model to summarize important performance metrics for the comparison with HOMER Pro's results.

After the comparison and its results, an improved version of the simulation tool HY4RES V2 is designed and tailored to this case study. In the second part of this work, it is used to analyze the optimal system composition and compare the separate systems to a combined one.

2.3 Input data for model comparison

With the overarching goal of comparing the HY4RES model's results with the one from HOMER Pro, the input data is prepared to resemble the one used in HOMER Pro as close as possible. If not indicated otherwise in the following chapters, the same approach and assumptions are taken. There were some misinterpretations of available data and no access to the Energy Management System (EMS) of the site for the HOMER Pro simulation. This induces several limitations to the interpretation of the results of this comparison these are presented in subsection 2.5. Accordingly, the input parameters for the second part of this work in HY4RES V2 are different and presented in subsection 2.6. February 29th is not included in the data. The following sections present the parameters and input data for each of the loads and generation technologies. Additionally, some information on energy storage systems and financial parameters is given.

2.3.1 Fish processing facilities

A mistake was made for the input of the load data of Island Seafoods in HOMER Pro. The grid feed-in from the wind turbine was accidentally mistaken as the load of the fish processing facility. Hence, the same approach is adapted for this part of the project for comparative reasons. The available grid feed-in by the wind turbine for each 15 min of the year 2023 is used as the quarter hourly load of the fish processing facility. The data is combined to express the electric load for each hour of the same year. As there is no recorded consumption data for Albatross Seafoods, it is assumed that its consumption is 0.9292 of Island Seafoods' [14]. With this approach, the combined load at the primary site can be computed and is available as an input to the HY4RES model.

2.3.2 Waste water treatment plant

In HOMER Pro a commercial electricity consumption profile from the library with $1200\,\frac{\text{kWh}}{\text{day}}$ and 430.72 kW peak is used [14]. As the profile itself is unknown, a fixed hourly load of 50 kW, which corresponds to the same daily consumption, is assumed for HY4RES throughout the year.

2.3.3 Wood drying kiln

As a means of utilizing excess energy from the wind turbine that can't be fed into the grid due to feed-in restrictions, a wood drying kiln was installed at the primary site in

2024. The typical primary wood, used for drying in Ireland is Sitka spruce with a density of $400 - 500\,\frac{\text{kg}}{\text{m}^3}$. It is assumed that 2000 kWh are needed to dry 1 t of Sitka spruce [15]. The installed kiln for the drying of this wood has a rated power of 300 kW. With the annual excess electricity from HOMER Pro's base case, the amount of wood dried can be computed. Hence, 1.8 t of wood can be dried per day considering a 12 h operation of the drying kiln. This results in 657 t of dried wood per year. An operation of 12 h per day between 08:00 a.m. to 08:00 p.m. with a constant power of 300 kW is assumed for every hour of the year. This is a simplified approach and can be later extended to simulate the biomass drying kiln as a flexible load which depends on the excess wind turbine generation. In HOMER Pro, a load with $3600\,\frac{\text{kWh}}{\text{day}}$ and 516.86 kW peak is chosen to represent the biomass drying kiln [14].

2.3.4 Small hydro power plant

On the secondary site, an SHP was installed in 2007. It utilizes the river flow and has the parameters shown in Table 1. Due to an installation error, it does not operate at rater power but only at 250 kW. It directly supplies the load of the WWTP and feeds excess electricity directly to the grid.

Table 1: Parameters of the SHP at the secondary site.

Name	Value	Note
P_r	380 kW	Only operates at 250 kW due to installation error
Type	Francis	
H_b	61 m	
n	1000 rpm	
Q	$0.7\,\frac{\text{m}^3}{\text{s}}$	
η_T	80 %	Turbine efficiency
η_Elec	95 %	Electric conversion

According to the Power Purchase Agreement (PPA), 15 min generation data for the year 2023 is available for the SHP. The same approach for data consolidation as for the fish processing facilities is repeated for the data of the SHP. For certain timestamps, data was missing or too many timestamps recorded. In this case, the surplus timestamp data was added to another timestamp where the load is zero, to reach the correct yearly total. Even though this is done with attention to detail, an error of 0.0061 % persists for the yearly total. In HOMER Pro a different approach was chosen. The SHP is modeled in the program directly with the data from Table 1 and a design flow rate of $0.522\,\frac{\text{m}^3}{\text{s}}$ to reflect the limited power of 250 kW [14].

2.3.5 Wind turbine

A single Vestas V52-850 wind turbine was commissioned in 2021. It is directly connected to the primary site's electrical network, supplying the demand of the two processing facilities and feeding excess electricity into the grid. Due to feed-in limitations, the turbine is only allowed to feed in 120 kW. The key parameters of the turbine are found in Table 2.

Table 2: Parameters of the Vestas V52 850 wind turbine at the primary site.

Name	Value	Note
P_r	850 kW	Maximum operation at 500 kW due to grid injection limitations
h_{hub}	44 m	
h_{alt}	60 m	above sea level
Lat.	54.673	
Long.	−8.422	
Data	merra2	for 2023

The simulation in HOMER Pro disregards the feed-in limit of the Vestas V52 wind turbine and simulates with the nominal power of 850 kW. The same is done in HY4RES. HOMER Pro uses an internal wind turbine simulation where the turbine model and wind profile are used. Wind data is loaded from NASA's POWER data base with 30 year mean hourly wind speeds. These are then scaled to $\bar{u}_{hub} = 6.4\,\frac{m}{s}$ as a yearly average. For the wind generation in HY4RES, data from Table 2 is inserted to Renewables.Ninja's wind simulation tool to receive the hourly generation data for the year 2023 [16]. To begin with, the hourly wind speeds were scaled to achieve $\bar{u}_{hub} = 6.4\,\frac{m}{s}$, the same value that is used in HOMER Pro. However, this lead to a much lower annual energy generation of 1,683,882 kWh. Therefore, it is decided to scale the hourly wind speeds for an annual energy generation of 2,240,471 kWh, the same annual generation that resulted from the HOMER Pro simulation. To adjust the hourly generation data of the wind turbine, the power coefficient is necessary. As it is a function of the wind speed it has to be computed for each hourly wind speed. Publicly available data [17] for the Vestas V52 is used and a polynomial regression created as shown in Figure 2. With the help of the plot, a polynomial regression of 6th order was created and hence the power coefficients for any wind speed can be computed. The regression function is found in Equation 1, its polynomial parameters are displayed rounded. However, during the simulation no rounding is applied. With Excel's goal seek function, the annual energy generation is adjusted to the corresponding value by multiplying the initial wind speeds from Renewables.Ninja with a multiplier of ≈ 0.79744156. This adjusts the annual energy generation to the desired value by adjusting the hourly wind speeds, getting as close as possible to the simulation of HOMER Pro.

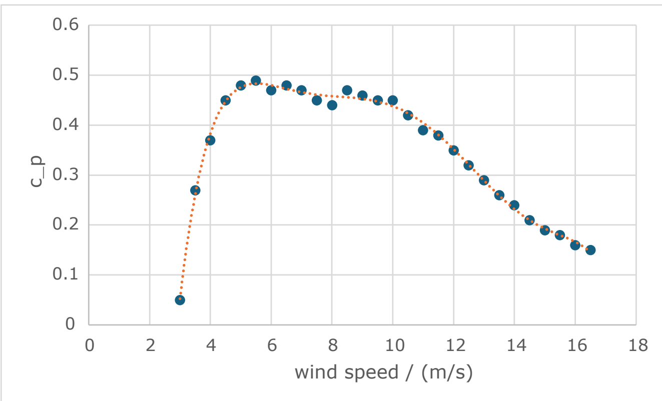

Figure 2: Vestas V52 850 kW power coefficient. Orange is polynomial regression of 6th order. Data from [17].

$$c_{\text{p}} = -7.3 \cdot 10^{-6}u^6 + 0.00047u^5 - 0.01215u^4 + 0.16063u^3 - \\ - 1.14862u^2 + 4.21017u - 5.70269 \quad (1)$$

2.3.6 Solar PV

To simulate the PV system, PVGIS 5.3 [18] is used with the input displayed in Table 3 to generate hourly electric energy values. PVGIS is run with a 1 kW_p nominal power, it's generation is then scaled to 120 kW_p in Excel. To align with the other input data, February 29$^{\text{th}}$ is removed. Due to availability restrictions, the year 2020 is used for the PVGIS simulation. Both slope and azimuth angle were optimized automatically by PVGIS.

Table 3: Parameters of the rooftop PV system.

Name	Value	Note
P_r	120 kW	(c-Si)
β	42 °	Slope
γ	0 °	Azimuth
f_derate	14 %	System losses
h_alt	46 m	above sea level
Lat.	54.673	
Long.	−8.422	
Data	PVGIS-SARAH2	for 2020

2.3.7 Biomass generator

To utilize only parts of the dried wood in a Biomass-gasifier ICE (BG) on site, a 25 kW generator is chosen. Therefore, still leaving dried wood to be sold on the local market. It is assumed that the 25 kW are constantly available throughout each hour of the year, amounting to a yearly energy generation through biomass of 219,000 kWh [14].

2.3.8 Energy storage

When the scenario to be compared encompasses a BESS, it is decided to use the nominal capacity of the BESS as an input in HY4RES. HOMER Pro uses a more sophisticated BESS simulation and regards the usable capacity. This is done for any scenario where a BESS is present. If not stated otherwise, Li-ion BESS are used.

2.3.9 Financial parameters

To achieve similar results in terms of cash-flows, the electricity feed-in price and purchase price from HOMER Pro are used [14]. These are 0.195 $\frac{€}{\text{kWh}}$ and 0.3808 $\frac{€}{\text{kWh}}$, respectively. They remain constant throughout each hour of the year.

2.4 Comparison with HOMER Pro

According to the simulations done in HOMER Pro, the same scenarios are created in the HY4RES model for comparison. The included technologies and scenarios are listed in Table 4. Furthermore, the approach for each simulated scenario in HY4RES is explained in more detail. As only primary and secondary site results are available from the HOMER Pro simulation, it is decided to look at the combined site only in the HY4RES V2 simulation.

Table 4: Technologies included in each scenario of the Primary and Secondary systems.

Scenario	Grid	Wind	SHP	BG	PV	BESS
Primary site						
Base Case	Yes	Yes	No	No	No	No
Scenario 1	Yes	Yes	No	Yes	No	No
Scenario 2	Yes	Yes	No	Yes	Yes	No
Scenario 3	No	Yes	No	Yes	No	Yes
Scenario 4	No	Yes	No	Yes	Yes	Yes
Scenario 5	No	Yes	No	No	Yes	Yes
Scenario 6	Yes	Yes	No	No	Yes	No
Secondary site						
Base Case	Yes	No	Yes	No	No	No
Scenario 1	Yes	No	Yes	No	Yes	No
Scenario 2	No	No	Yes	No	No	Yes

Primary site: Base Case

In the base scenario, the combined hourly loads of Island Seafoods and Albatross Seafoods are inserted into the HY4RES model together with the adjusted hourly wind generation, as discussed in subsection 2.3. The simulation is run in the Excel sheet and results are extracted as graphs and key performance indicators. Although Figure 1 already includes the wood drying kiln, the Base Case of the Primary site does not. This is to align with HOMER Pro's simulation.

Primary site: Scenario 1

In terms of the excess electricity, available for the biomass drying kiln, the value from HOMER Pro's simulation is used for the purpose of comparison. The hourly load profile from the base case is used and the one from the biomass drying kiln added. This new profile is then inserted into the HY4RES model. Additionally, the hourly generation profile of the biomass generator is added.

Primary site: Scenario 2

Scenario 1 is simply extended by the solar PV generation as discussed in subsection 2.3.

Primary site: Scenario 3

As this scenario is off-grid, only having a BESS to balance energy deficit or excess, the sum of hourly deficits after the operation of the BESS is subtracted from the annual consumption. Leaving only the met electricity consumption. According to the value, the reduction in annual consumption of the wood drying kiln can be deducted as well as the reduction in annually dried wood. To achieve an acceptable amount of unmet electricity demand, a BESS with capacity of 22 MWh is chosen [14].

Primary site: Scenario 4

The same approach is taken as for Scenario 3, only extending the generation by solar PV.

Primary site: Scenario 5

This scenario does not include the BG. However, it still has the wood drying kiln as a load. The wood is simply not consumed on site, but sold on the local market. According to [14], the same percentage of unmet electricity demand is used as in Scenario 4. Hence, this reduction in electricity demand is translated into less electricity being available for drying the wood, hence reducing the amount of wood that can be dried per year and the hourly electricity demand. The reduced hourly demand is then added to the fish processing facilities' hourly loads and the final vector inserted in the HY4RES tool. To achieve the same percentage of unmet electricity demand, a BESS with a capacity of 63 MWh is needed [14].

Primary site: Scenario 6

Returning to a grid-tied system, the standard consumption profile of the wood drying kiln is regarded again, 657 t of wood are dried each year. As such no energy deficit is noted and a cash-flow can be recorded.

Secondary site: Base Case

For the secondary case, the column of the tertiary generation technology is filled with the hourly generation data of the SHP and the hourly load profile of the WWTP inserted in the electrical consumption column.

Secondary site: Scenario 1

For this scenario, the base case is simply extended by the rooftop solar PV system and its hourly generation vector inserted in the HY4RES tool.

Secondary site: Scenario 2

Instead of the grid-tied system, this scenario includes a 400 kWh BESS. According to [14], this does not fully meet the electricity demand during the summer months where hydropower generation is low.

2.5 Limitations of comparison

Both models, HOMER Pro and HY4RES, have their limitations. In terms of the HY4RES model, the cash-flow computation leads to a very limited significance of the result as it only includes the cash-flow with the grid and completely disregards any investment cash-flows or other operational cash-flows. Additionally, the simplified BESS simulation, disregarding charge/discharge efficiencies or charge/discharge power, does not allow for accurate modeling. HOMER Pro's simulation is held back by a simplified hydropower generation profile which does not differentiate between different hourly power outputs but only between months, keeping the monthly hourly power output constant for each month. Using already available load profiles from the HOMER Pro library can lead to deviations from reality, but are a better estimate than assuming constant load profiles.

Secondly, there are limitations induced by the input data used for the HOMER Pro simulation. After reviewing the parameters of the WWTP, it becomes evident that the HOMER Pro load profile used has daily electricity consumption is 4.68 times higher than the actual daily consumption metered on site. Hence, the input data for both simulations does not reflect reality. However, using a constant hourly load in HY4RES also induces an error that can be substantial compared to the real load profile. The load of the biomass drying kiln, which should be flexible and only operate when excess electricity is available, was considered constant for the hours of operation during the day. Using the annual excess electricity from the Primary Site: Base Case for a basis of the constant hourly load calculation is flawed. This has the effect of increasing the energy deficit and as such also the expenses from purchasing electricity from the grid. This only allows comparisons between scenarios that include the biomass drying kiln, not with the base case or other scenarios. Hence, the results can not be taken as absolute values. After some further investigation, it became clear that the vector which was supposed to represent Island Seafoods' hourly loads actually is the amount of excess electricity from the wind turbine being sold to the grid under a flexible price PPA. The downscaling of the wind turbine generation data to the average annual hourly wind speed is done according to a value that was estimated by an engineering consultancy before the installation of the turbine and hence comes with uncertainty about its applicability. Additionally, HOMER Pro disregards the grid injection limit which would lead to a reduced grid cash-flow in both models. In HOMER Pro the costs of equipment which was already bought and installed several years ago — the sunk cost — was included in the financial calculation. This renders the results of the financial calculation useless in terms of real financial benefits of a scenario, it only allows for a comparison between scenarios.

2.6 HY4RES V2

Taking the learnings from the previous comparison into account and the model's limitations, a new model is designed from scratch to fill the missing gaps and provide a more realistic simulation of the case study. Several misinterpretations of the input data were discovered which are also corrected for the simulation of this model. The goal is to provide a techno-economic assessment tool which takes existing hybrid renewable energy systems into account and provides a detailed analysis and optimization to expand the system with additional technologies. Each of the individual sites is assessed with the tool and then also the combined site. All three systems are optimized in terms of maximizing NPV while the combined site is additionally optimized for maximizing Self-Sufficiency Ratio (SSR). The following chapters summarize the input data used for the new model, the model itself in terms of technical and financial modeling and the optimization techniques applied.

2.6.1 Input data

2.6.1.1 Fixed loads

The hourly load profile for 2023 of both seafoods processing facilities is available from their EMS. For the WWTP an exact hourly load profile is not available as its consumption is not yet metered consistently. During one week in winter 2023, the consumption was analyzed. The WWTP operates 24 h per day and seven days per week. It shows an average hourly consumption of 10.68 kWh with a peak load of 26 kW. As a simplification a hourly load profile for one day is created with the corresponding peak load and average, mentioned above. This is presented in Table 5. It is assumed that this daily load profile is representative for all days of the year. Then, one combined hourly load profile for Island Seafoods, Albatross Seafoods and the waste water treatment plant is created for the year 2023 and loaded into the model.

Table 5: Created load profile for the WWTP, according to the metered peak demand and hourly average load.

Hour	P_{WWTP} / kW	Hour	P_{WWTP} / kW
1	4	13	22
2	4	14	26
3	4	15	22
4	4	16	16
5	6	17	14
6	8	18	11
7	10	19	9
8	11	20	8
9	12	21	6
10	14	22	4
11	16	23	4
12	18	24	4

2.6.1.2 Flexible load

If not indicated otherwise, the same parameters are used as for the comparison, presented in subsubsection 2.3.3. Roadside raw wood with a moisture content of 45-60 % [19] is bought from the local market. The wood drying kiln dries sitka spruce chips to a moisture content of 20 % [20] which results in a Lower Heating Value (LHV) of $LHV_{\mathrm{wood}} = 3811\,\frac{\mathrm{kWh}}{\mathrm{t}}$ [21]. The installed kiln for the drying of wood has a rated power of $P_{\mathrm{r,kiln}} = 300\,\mathrm{kW}$. For simplification, it is assumed that the kiln operates between 200 kW and 300 kW. Hence, at every hour of the year where renewable excess electricity is available and above 200 kW a certain amount of wood can be dried. Its operation is mathematically explained in Equation 2, where each power P is specific for one hour of the year.

$$
\begin{aligned}
&if\, P_{\text{wind}} + P_{\text{SHP}} + P_{\text{PV}} - P_{\text{load,fixed}} \geq 200\,\text{kW} \rightarrow P_{\text{kiln}} = P_{\text{wind}} + P_{\text{SHP}} + P_{\text{PV}} - P_{\text{load,fixed}} \\
&if\, P_{\text{wind}} + P_{\text{SHP}} + P_{\text{PV}} - P_{\text{load,fixed}} \geq 300\,\text{kW} \rightarrow P_{\text{kiln}} = 300\,\text{kW} \\
&else\, P_{\text{kiln}} = 0\,\text{kW}
\end{aligned} \tag{2}
$$

The dried wood output of the drying kiln is computed according to Equation 3, where P_{kiln} corresponds to the power of the drying kiln at the hour observed.

$$
m_{\text{wood,dried}} = \frac{P_{\text{kiln}}}{2000\,\frac{\text{kWh}}{\text{t}}} \tag{3}
$$

An additional vector is defined, $m_{\text{wood,dried,cum}}$ which sums all the previous hours of the year to the current one. If desired, an initial amount of wood $m_{\text{wood,dried,t0}}$, left in the storage from the previous year, can be added to this cumulative vector. It is assumed that $m_{\text{wood,dried,t0}} = 0\,\text{t}$. Surplus production of dried wood is sold at the market price, indicated in Table 7. The wood purchase and selling prices are adjusted to the reduction of the moisture content. Hence, the wood cash-flow can directly be computed with the amount of dried wood not used in the BG.

2.6.1.3 Small hydro power plant

Generation data from the fixed PPA contract is available in 15 min time stamps for the year 2023. As the total generation is not known and neither is the percentage of self-consumption of the SHP, this data is used as the total generation before feed-in. The 15 min data is consolidated into hourly values.

2.6.1.4 Wind turbine

The parameters from Table 2 are inserted into Renewables.Ninja's wind simulation tool to receive the hourly generation data for the year 2023 [16]. No scaling of the generation output is done at this point.

2.6.1.5 Solar PV

To simulate the PV system, PVGIS 5.3 [18] is used with the input displayed in Table 3. PVGIS is run with a $1\,\text{kW}_\text{p}$ nominal power, it's generation is then scaled in the model by multiplying the P_{PV}, set by the optimization technique, with the hourly generation vector from PVGIS. The approximation of [14] is used to limit the PV system to the roof of the seafood processing facilities which can host up to 120 kW installed power.

2.6.1.6 Biomass generator

In order to make use of the dried wood on site, a BG is proposed. The objective of this optimization is to find the suitable rated power for the BG, to support the renewable system as a base load throughout the year. It is decided to chose a gasifier-ICE-generator unit due to its efficient conversion path and sizing options, which range from a few kW_e to several hundreds kW_e. As a first step in such a BG, the wood chips are gasified in a downdraft gasifier. Afterwards, the syngas is combusted in a gas engine after cleaning and cooling [22]. In terms of efficiency, a total wood to electricity conversion efficiency of $\eta_{\mathrm{BG}} = 25\,\%$ [23] is assumed according to Gonzalez et al.'s simulation [24]. In terms of operation, the renewable sources will have priority to supply the load and the BG is only activated, if the loads can't be fully supplied by the generation of the wind turbine and SHP as outlined in Equation 4. Additionally, the wood consumption of the BG is tied to the biomass dried on site, no additional dried wood chips are bought from the market for its operation. To keep its efficiency as high as possible, it only operates at its rated power. The BG is not set up to supply the flexible load of the wood drying kiln, only the fixed loads.

$$P_{\mathrm{wind}} + P_{\mathrm{SHP}} + P_{\mathrm{PV}} < P_{\mathrm{load,fixed}} \wedge m_{\mathrm{wood,dried,cum}} \geq m_{\mathrm{wood,BG}} \tag{4}$$

$m_{\mathrm{wood,BG}}$ is the amount of wood needed to operate the BG at the defined power. It is computed according to Equation 5.

$$m_{\mathrm{wood,BG}} = \frac{P_{\mathrm{BG}}}{\eta_{\mathrm{BG}} \cdot LHV_{\mathrm{wood}}} \tag{5}$$

2.6.1.7 BESS

As a BESS, a Lithium-ion battery system is assumed. The input parameters for the BESS are found in Table 6. The Energy-to-Power Ratio (EPR) of the BESS is equal to a storage duration of 4 hours [25]. Additionally, State of Health (SOC) limits are set to avoid deep discharge of the battery and have an initial charge at the first timestamp of the simulation. The optimization technique sizes the BESS in terms of its capacity C_{BESS} in the unit kWh.

Table 6: Parameters of the BESS.

Name	Value	Note
EPR	$4\,\frac{\mathrm{kWh}}{\mathrm{kW}}$	equals 4 h storage duration
$\mathrm{SOC}_{\mathrm{t0}}$	$0.25 \cdot C_{\mathrm{BESS}}$	
$\eta_{\mathrm{ch/dis}}$	0.95	Same efficiency for charging and discharging assumed
$\mathrm{SOC}_{\mathrm{min}}$	$0.1 \cdot C_{\mathrm{BESS}}$	

According to Equation 6, the charge/discharge power P_{BESS} of the battery is computed. This is used to limit the amounts of energy being charged and discharged at each hour and is also used to compute the CAPEX and OPEX of the BESS.

$$P_{\mathrm{BESS}} = \frac{C_{\mathrm{BESS}}}{EPR} \tag{6}$$

The charge and discharge modeling is found in Figure 3. It is done accordingly for each hour of the year. The resulting charge and discharge powers are to be seen from the system point of view — the power, the system has available to charge the battery or the power it gets from discharging the battery. Hence, the power values do not represent the actual energy that is stored in the battery. $\eta_{\text{ch/dis}}$ is only considered for the computation of the battery SOC. The latter is computed as shown in Equation 7 where SOC^{t-1} is the SOC of the previous timestamp. The SOC is generally given in kWh. Thanks to the charge and discharge modeling, it never exceeds the battery capacity C_{BESS}, nor does it reach a value below SOC_{min}.

$$SOC^t = SOC^{t-1} + P^t_{\text{ch}} \cdot \eta_{dis} - \frac{P^t_{\text{dis}}}{\eta_{ch}} \tag{7}$$

Once the annual electricity charged and discharged is known, the number of full charge/discharge cycles can be computed according to Equation 8. The corresponding number of years is computed by dividing the number of lifetime cycles from Table 7 by the actual number of cycles per year $n_{\text{BESS}} = \frac{n_{\text{BESS-cycles}}}{5475}$. The lifetime of the battery is then evaluated according to the shorter lifetime, either the one derived from the cycles or the calendar life from Table 7.

$$n_{\text{BESS-cycles}} = \frac{\sum E_{\text{a,ch}} + \sum E_{\text{a,dis}}}{2 \cdot C_{\text{BESS}}} \tag{8}$$

2.6.1.8 Grid

The system is grid connected, as depicted in Figure 1. However, due to grid capacity restrictions, there is a feed-in limit of 120 kW at the primary site for the wind turbine. For this project, it is assumed that this limitation is valid for the combined site and primary site. The SHP has an hourly feed-in tariff according to a fixed PPA which is shown in Table 7. For the electricity purchase prices, the facility has fixed night and day tariffs. Between 11:00 p.m.-07:00 a.m. it is at 0.1477 $\frac{€}{\text{kWh}}$, while it lies at 0.2393 $\frac{€}{\text{kWh}}$ for the rest of the day. These tariffs are obtained from the EMS of the site. For the primary site, the feed-in tariff is equal to the electricity purchase price and has the same hourly variation through the day. This variable feed-in tariff is also applied in for the combined site.

2.6.1.9 Financial parameters

All input parameters for the financial calculation are found in Table 7. The system lifetime is set to 25 years in the financial analysis according to similar studies [24]. Adhering to the Irish Tax rules, any renewable energy technology is depreciated linearly over 8 years, regardless of its lifetime [26]. According to [27], the market value of a BG based on downdraft gasifier technology is 15 % of it's original CAPEX cost for a 20 years lifetime. To use a conservative value and adjust the lifetime to 25 years, a market value of 10 % is assumed. For simplification purposes it is assumed that neither the PV system nor the BESS has a market value at the end of their lifetime. To account for the decreasing price of BESS and PV along the project's lifetime, negative inflation rates for the CAPEX cost, in case of a reinvestment, are considered.

In terms of a carbon tax in Ireland, biomass that is solely used for electricity generation and adheres to certain criteria is fully exempt. These criteria include meeting the sustainability requirements of the Renewable Energy Directive (RED II) by the European

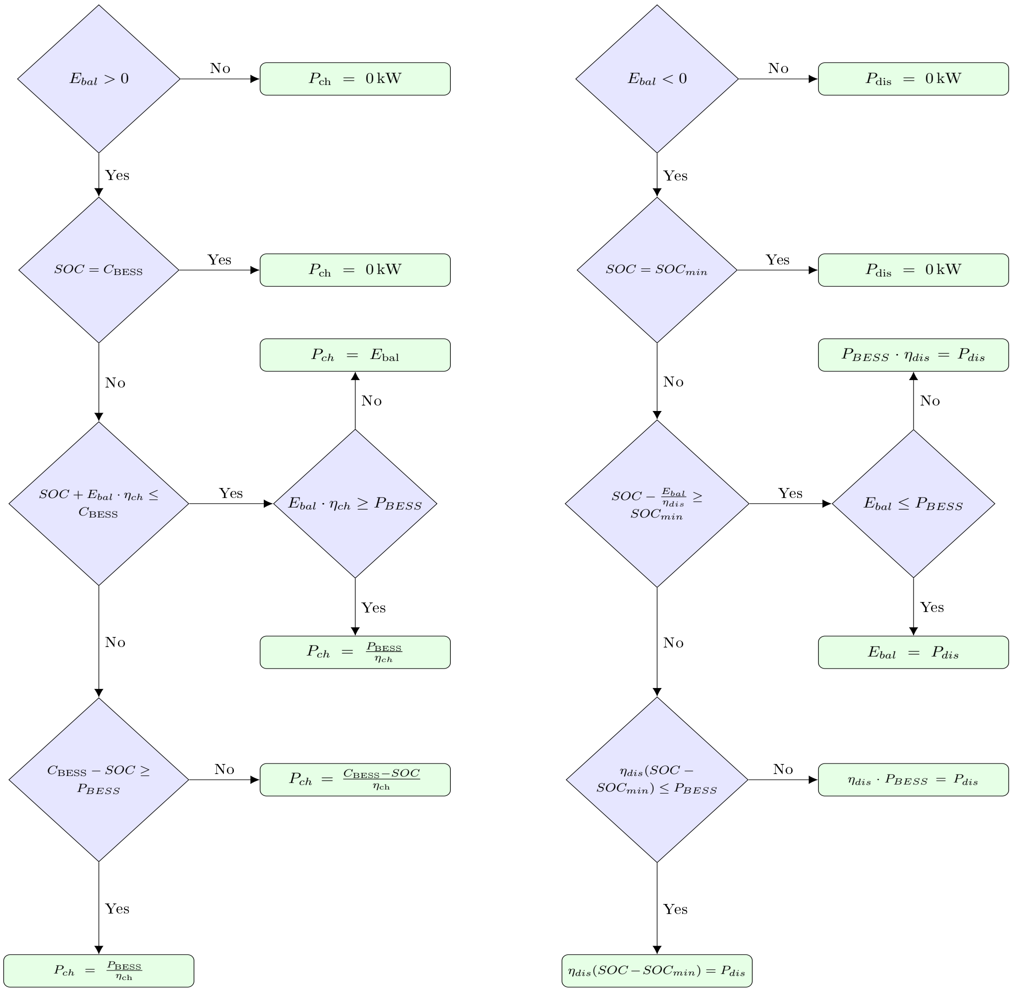

(a) BESS charge modeling.

(b) BESS discharge modeling.

Figure 3: Flow-charts of the BESS charge and discharge modeling in HY4RES V2.

Union and having compliance documents available for inspection. This exception is expanded to biomass Combined Heat and Power (CHP) plants with high efficiency [28, 29]. Hence, the carbon tax on the CO_2 emissions from the biomass generator are set to $0\,\frac{€}{\mathrm{t\,CO_2\,eq}\cdot}$. However, the model allows an adjustment of this parameter to other regions and case studies.

2.6.1.10 Emission parameters

In terms of carbon emissions, it is decided to regard the carbon emissions of operation, not life-cycle emissions. Hence, the ones related to the biomass conversion and grid electricity supply. Table 8 shows the emissions' parameters for these two sectors. The emissions related to the biomass conversion are taken from [39], selecting the emissions related to wood chips from UK sustainably managed broadleaf forests. The yearly total emissions are computed by multiplying the annual energy purchased from the grid or generated by the BG and multiply it with the corresponding emissions data from Table 8.

Table 7: Cost and financial parameters.

Data	Variable name	Value	Source
Lifetime			
System lifetime	n	25 years	[24]
BG lifetime	n_{BG}	25 years	[24]
PV modules lifetime	n_{PV}	25 years	[30]
PV converter lifetime	$n_{\text{PV-c}}$	15 years	[31]
BESS calendar life	n_{BESS}	15 years	[25]
BESS cycle life	n_{BESS}	5475 cycles	[25]
Financial data			
General inflation rate	g	3 %	[24]
Corporate tax rate	TR	12.5 %	[26]
Discount rate	r	6 %	[32, 33]
PV converter inflation rate	g_{PV}	-5 %	[34]
BESS inflation rate	g_{PV}	-5.7 %	[25]
Capital costs			
BG capital cost	I_{BG}	6,000 $\frac{€}{\text{kW}}$	[14]
BG market value at end-of-life	MV_{BG}	$0.1 \cdot I_{\text{BG}}$	[27]
PV capital cost	I_{PV}	1,500 $\frac{€}{\text{kW}}$	[35]
PV market value at end-of-life	MV_{PV}	0	
PV converter capital cost	I_{PV}	150 $\frac{€}{\text{kW}}$	[35]
PV converter market value at 15 years	$MV_{\text{PV-c}}$	0	
BESS capital cost power	I_{BESS}	2,749.83 $\frac{\$}{\text{kW}}$	[25]
BESS market value at 15 years	MV_{BESS}	0	
Fixed O&M costs			
BG fixed O&M costs	$C_{\text{O\&M,BG}}$	0.12 $\frac{I_{\text{BG}}}{\text{year}}$	[36]
PV fixed O&M costs	$C_{\text{O\&M,PV}}$	28.91 $\frac{€}{\text{kW}}$	[24]
BESS fixed O&M costs	$C_{\text{O\&M,BESS}}$	$0.025 \cdot I_{\text{BESS}}$	[25]
Variable O&M costs			
BG variable O&M costs ($P_{\text{BG}} \leq 100\,\text{kW}$)	$c_{\text{O\&M,BG}}$	0.18 $\frac{€}{\text{kWh}}$	[37]
BG variable O&M costs ($P_{\text{BG}} > 100\,\text{kW}$)	$c_{\text{O\&M,BG}}$	0.12 $\frac{€}{\text{kWh}}$	[37]
Subsidies			
PV investment grant ($P_{\text{PV}} \leq 20\,\text{kW}$)	s_{PV}	300 $\frac{€}{\text{kW}}$	[38]
PV investment grant ($P_{\text{PV}} \leq 200\,\text{kW}$)	s_{PV}	200 $\frac{€}{\text{kW}}$	[38]
PV investment grant ($P_{\text{PV}} \leq 1000\,\text{kW}$)	s_{PV}	150 $\frac{€}{\text{kW}}$	[38]
Wood prices			
Roadside wood pulp price	$p_{\text{raw,wood}}$	40 $\frac{€}{\text{t}}$	[19]
Dried wood chips	$p_{\text{dried,wood}}$	120 $\frac{€}{\text{t}}$	[19]
Grid financial data			
SHP fixed PPA price	$p_{\text{SHP,PPA}}$	0.0946 $\frac{€}{\text{kWh}}$	
Carbon tax			
Carbon tax on biomass conversion	$p_{\text{carbon-tax}}$	0 $\frac{€}{\text{t}\,\text{CO}_2\,\text{eq}\cdot}$	[28, 29]

exchange rate applied 1 € = 1.1292 $

Table 8: Carbon emissions parameters for the biomass conversion and electricity from the power grid.

Data	Variable name	Value	Source
Emissions from biomass conversion	$m_{CO_2\,eq.,BG}$	$69\,\frac{g\,CO_2\,eq\cdot}{kWh}$	[39]
Emissions from grid electricity	$m_{CO_2\,eq.,grid}$	$187\,\frac{g\,CO_2\,eq\cdot}{kWh}$	[40]

2.6.2 Simulation

This chapter explains how HY4RES V2 simulates energy flows and conducts the financial analysis. The combined site is used exemplary as it shows all the technologies implemented in both primary and secondary site. Hence, it is also valid for the latter two. Figure 4 provides a good overview of the technical part of the model in Excel. To begin with, the hourly load profiles and generation profiles from the wind turbine and SHP are loaded into the model. Additionally, all the input parameters are inserted. Finally, the PV installed power, BG installed power and BESS capacity must be defined or optimized by Solver. According to the selected PV installed power, the hourly generation profile is created. The total generation is compared with the fixed load profile. In case of an energy excess large enough to operate the wood drying kiln, its load is subtracted from the balance for the corresponding hour. With the energy consumed by the kiln, the amount of dried wood is computed. Afterwards, the operation of the BG is validated and its generation added to the balance. As a final step, the BESS operation is applied. Any energy deficit that can not be covered by the system or the BESS is purchased from the grid. On the other hand, any excess after fully charging the BESS is sold to the grid at the hourly feed-in tariff. The energy being sold to the grid is compared with the feed-in limitation of 120 kW. In case that the excess is above the limit, only 120 kW can be sold to the grid, the rest is wasted. It is assumed that this loss is balanced through the power electronic converters of the wind turbine and PV system.

With these hourly parameters calculated, some key performance indicators for the year can be computed. Among them being the SSR of the system — indicating the grid independence of the system. It is calculated as shown in Equation 9. In the equation E_a is the annual electricity generated or consumed.

$$SSR = \frac{E_{a,loads} + E_{a,kiln} - E_{a,from\,grid}}{E_{a,loads} + E_{a,kiln}} \tag{9}$$

Additionally, the Self-Consumption Ratio (SCR) of the system — indicating the amount of renewable generation, directly consumed on site — is computed according to Equation 10. $E_{a,gen}$ corresponds to the sum of the renewable energy generated on site during the whole year.

$$SCR = \frac{E_{a,loads} + E_{a,kiln}}{E_{a,gen}} \tag{10}$$

An overview of the cash-flow simulation is given in Figure 5. However, it has to be noted that only differences in cash-flow compared to the base-line matter. The latter is considered as the system without the BG, PV or BESS. Hence, any differences in cash-flows that occur due to the integration of the new technologies are taken into account.

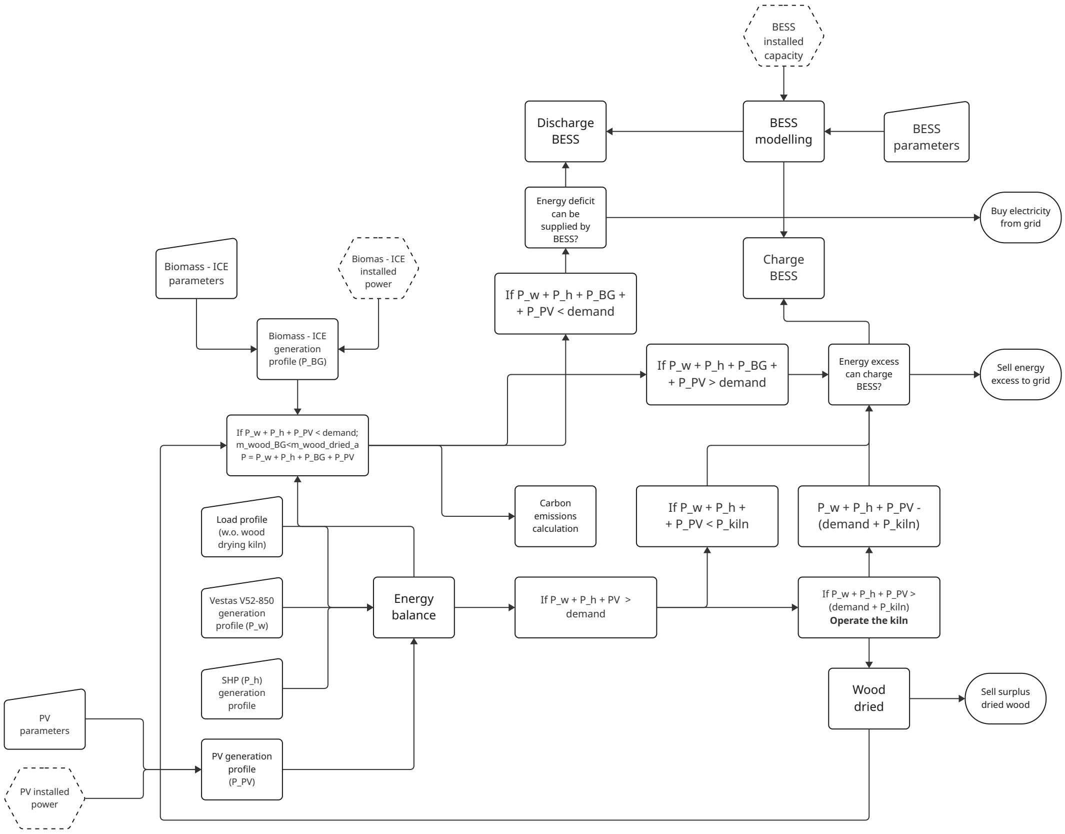

Figure 4: Flow chart of the technical simulation of the combined system. Dashed hexagons represent the decision variables for optimization.

To begin with, the Investment Cash-Flows (ICF) is computed according to Equation 11 for each of the 25 years, where RV is the residual value of the asset after its lifetime. Hence, the latter is only regarded in the last year of the project or the asset's lifetime, while the investment is only regarded in the first year and in case an reinvestment occurs due to an asset reaching its end of life before the project's lifetime ends.

$$ICF = -I_{\mathrm{PV}} + RV_{\mathrm{PV}} - I_{\mathrm{PV,conv}} + RV_{\mathrm{PV,conv}} - I_{\mathrm{BG}} + RV_{\mathrm{BG}} - I_{\mathrm{BESS}} + RV_{\mathrm{BESS}} \quad (11)$$

RV is computed according to Equation 12, where MV stands for the market value of the asset at the end of the project's lifetime and BV stands for the book value of the same asset in the last year of the project or the end of life of an asset. As the company profits from the higher market value, it has to pay corporate tax TR on the difference.

$$RV = MV - (MV - BV) \cdot TR \quad (12)$$

In a next step, the Operating Cash-Flows (OCF) is calculated. With the resulting dried wood and electricity purchased from the grid and fed into the grid, the wood and grid cash-flows are computed. The cash-flow from wood drying and selling can be calculated according to Equation 13. While the grid-cash flow is computed according to

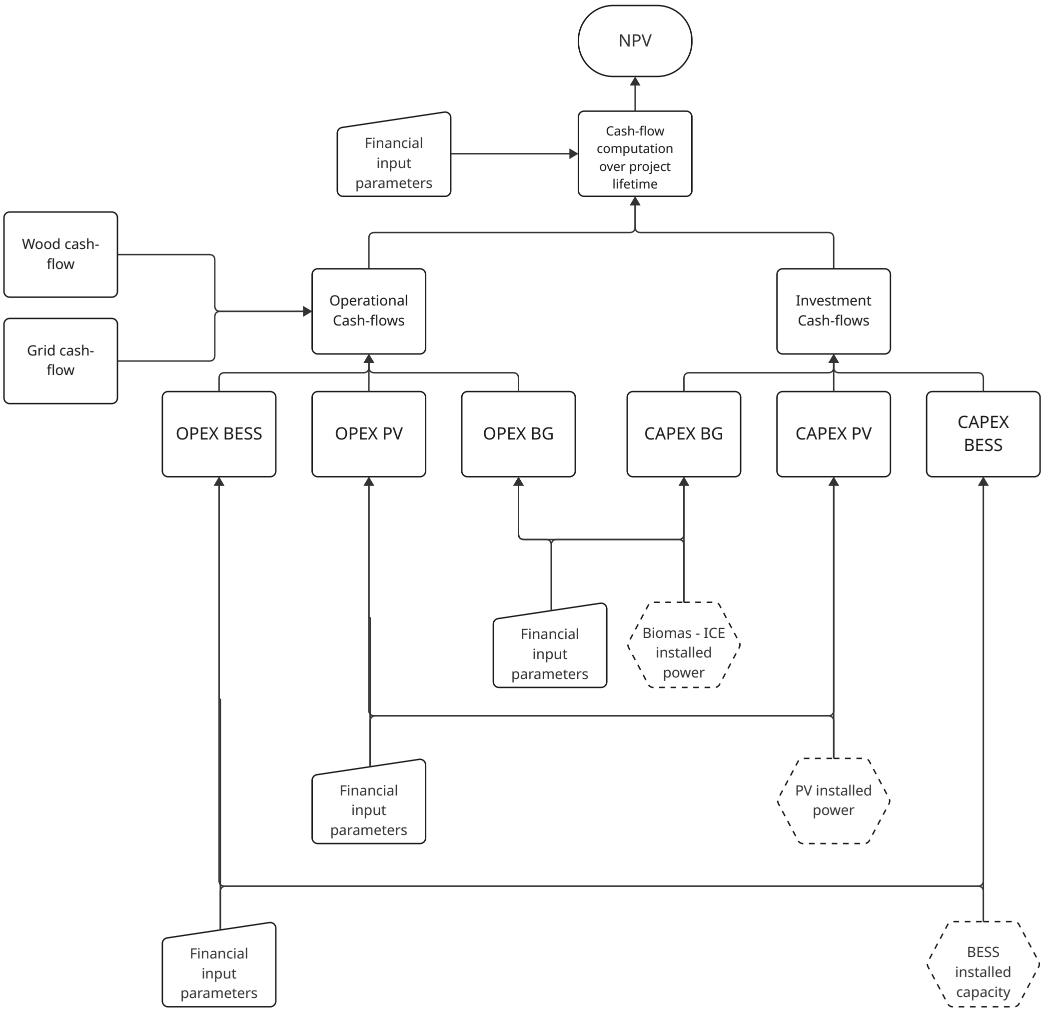

Figure 5: Flow chart of the financial simulation for the combined system. Dashed hexagons represent the decision variables for optimization.

Equation 14. This is done once for the baseline and then for the optimized system, the difference is then accounted for in the revenue calculation.

$$CF_{\text{wood}} = ((m_{\text{wood,dried}} - m_{\text{wood,BG}}) \cdot p_{\text{dried,wood}}) - m_{\text{wood,dried}} \cdot p_{\text{raw,wood}} \tag{13}$$

$$CF_{\text{grid}} = E_{\text{excess}} \cdot p_{\text{grid,sell}} - E_{\text{deficit}} \cdot p_{\text{grid,buy}} \tag{14}$$

Next, the cash-flow changes regarding the electricity sales and wood sales are computed for the first year. In order to take inflation into account, the annual cash-flow results from the technical simulation are compounded with the inflation rate to the corresponding year of the project. $\Delta Revenue = \Delta Electricity\, sales + \Delta Woodsales$ computes the change in revenue for the implementation of the BG, PV and BESS. The same approach is taken for the electricity purchased from the grid. The costs for purchasing wood are neglected as the amount of wood dried does not change due to the implementation of the BG, only the amount sold changes. According to the optimal sizing of the PV, BESS and BG the fixed and variable O&M costs are computed for the first year. Afterwards, they are compounded with the annual inflation rate to the remaining years of the project's lifetime. This leads to the change in cash-flows of expenses $\Delta Expenses = \Delta Electricity\, purchased + C_{\text{O\&M,BG}} + c_{\text{O\&M,BG}} + C_{\text{O\&M,BESS}} + c_{\text{O\&M,BESS}} + C_{\text{O\&M,PV}} + c_{\text{O\&M,PV}}$. The OCF is computed now according to Equation 15, where $EBITDA = \Delta Revenue - \Delta Expenses$. Depreciations are calculated according to paragraph 2.6.1.9.

$$\begin{aligned} OCF &= EBIT \cdot (1 - TR) + Depreciations = \\ &= (EBITDA - Depreciations) \cdot (1 - TR) + Depreciations \end{aligned} \tag{15}$$

Finally, the Free Cash-Flows (FCF) can be computed as $FCF = ICF + OCF$ and discounted to the present day with the discount rate r to get the Discounted Cash-Flows (DCF). The sum of these cash-flows gives the NPV, according to Equation 16, t is the corresponding year. It is a fitting metric to assess the viability of a project as it discounts cash-flows over the lifetime of the project to the current date and enables an evaluation on monetary terms in the present.

$$NPV = \sum_{t=0}^{25} \frac{FCF}{(1+r)^t} = \sum_{t=0}^{25} DCF \tag{16}$$

Additionally, the profitability index $PI = \frac{NPV}{I}$ can be calculated. Other metrics are also computed such as the Payback Period (PP), the LCOE and Modified Internal Rate of Return (MIRR). The MIRR is chosen instead of the Internal Rate of Return (IRR), as it is more accurate for projects where re-investments occur. It is computed according to Equation 17 where $FVCF^+$ is the future value of all positive cash-flows, $PVCF^-$ is the present value of all negative cash-flows and n is the year. In the Excel model, Excel's proprietary function for the MIRR is used.

$$MIRR = \sqrt[n]{\frac{FVCF^+}{PVCF^-}} - 1 \tag{17}$$

The $LCOE$ on the other hand is computed for each generation technology separately and can be derived from Equation 18, where the total costs over the project's lifetime is divided by the total energy generated by the technology over its lifetime while both are discounted to the present day.

$$LCOE = \frac{\sum_{t=0}^{25} \frac{C_{\text{O\&M}} + c_{\text{O\&M}} + I}{(1+r)^t}}{\sum_{t=0}^{25} \frac{E_{\text{a}}}{(1+r)^t}} \tag{18}$$

The computation of the PP is slightly more complex. It is defined as the time period until the accumulated DCF turn positive and in terms of this model is given in years. The corresponding mathematical description is given in Equation 19. It looks for the year p where the sum of DCF turns positive. $p - 1$ is the year prior to the year p.

$$
\begin{aligned}
&if \sum_{t=0}^{p} DCF > 0, t = min \\
&PP = t\left(\sum_{t=0}^{p} DCF > 0\right) + \left|\frac{DCF_{p-1}}{DCF_p}\right|
\end{aligned}
\tag{19}
$$

2.6.3 Optimization

The overall goal of this optimization project is to maximize the NPV of the project. With the implementation of the model in Excel, Solver only has a limited number of optimization techniques available. Simplex Linear Programming (LP) can be chosen for problems that are linear and smooth. As this optimization problem is non-linear, it can't be applied. Two other options are available, the Evolutionary method based on metaheuristics. It can be applied to any optimization problem, even if it is non-smooth and non-linear. The last option is an optimizer based on the Generalized Reduced Gradient (GRG) methodology for non-linear but smooth problems. It is based on simple derivatives of the fitness function and tries to find a solution by comparing the slope of the function as it changes the input parameters. This can directly lead to a local optimum but overlook the global one. Hence, it is decided to include the Multi-start option which starts at different points along the function and follows the most promising trend to find the global maximum. As the fitness function of the NPV is non-linear but smooth, both Evolutionary and GRG with Multi-start can be applied. Table 9 summarizes the key inputs for the optimization, objective function and decision variables. The upper boundary of 120 kW_p of the PV system correspond to the limited roof space available on the facility's buildings. The other two values are not restricted by the site requirements but rather by the input parameters which are only valid for a certain capacity or power rating of the BESS or BG. In order to assess a system which has the highest possible SSR, another optimization is done. The combined site is optimized with the objective function being to maximize the SSR.

Figure 6 provides an overview of the optimization process for the NPV. However, the same procedure is applied to optimize for SSR. The hexagons with the dashed lines display the decision variables.

2.6.4 Sensitivity analysis

After the optimization found the optimal size of the BG, PV and BESS, a sensitivity analysis is conducted on the most uncertain parameters. The same approach as taken by [24] is chosen where each of the parameters is changed by $\pm 10\,\%$ of its original value and the change in NPV and PP observed. The five input parameters on which the sensitivity analysis is conducted are the discount rate, each of the technology's investment costs, the electricity feed-in price, the electricity purchase price and the biomass-gasifier ICE unit's conversion efficiency.

Table 9: Fitness function, decision variables and optimization parameters for the Evolutionary method and GRG Multi-start.

Objective function	max NPV, max SSR
Decision variables	P_{PV}, C_{BESS} & P_{BG}
Constraints on PV	$0\,\mathrm{kW} \leq P_{\mathrm{PV}} \geq 120\,\mathrm{kW}$; $P_{\mathrm{PV}} = \mathrm{int}$
Constraints on BESS	$0\,\mathrm{kWh} \leq C_{\mathrm{BESS}} \geq 1000\,\mathrm{kWh}$; $C_{\mathrm{BESS}} = \mathrm{int}$
Constraints on BG	$0\,\mathrm{kW} \leq P_{\mathrm{BG}} \geq 500\,\mathrm{kW}$; $P_{\mathrm{BG}} = \mathrm{int}$

Value	Evolutionary	GRG
Convergence	0.001	0.001
Mutation rate	0.075	
Population size	100	100
Random seed	5	5
Time limit without improvement	30 s	
Require bounds on variables	✓	✓
Derivatives		Forward
Multi-start		✓

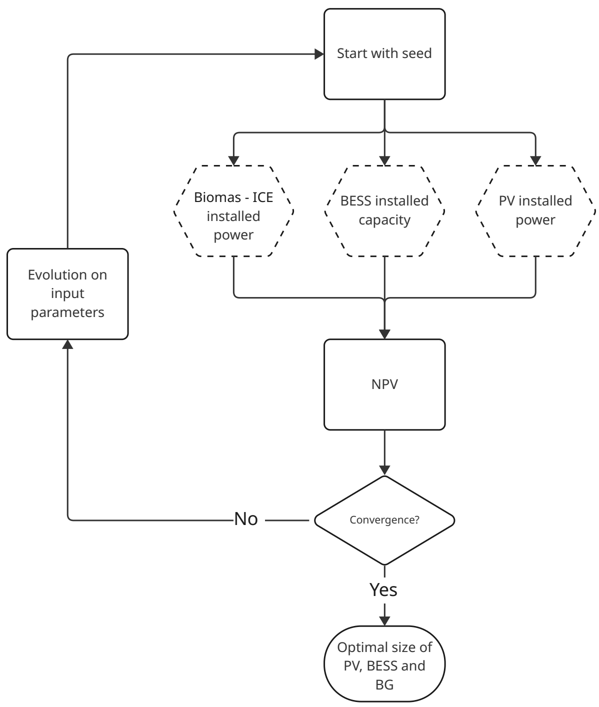

Figure 6: Flow chart of the optimization process.

3 Results

3.1 Comparison with HOMER Pro

3.1.1 Primary site

This section compiles the results for the primary site in terms of energy consumption, generation and cash-flow in Table 10, Table 11 and Table 12, respectively. All scenarios' results are summarized in the tables below, while the following sections present extended results for each individual scenario.

Table 10: Primary site: Comparing the electricity consumption values from HY4RES with HOMER Pro.

	HY4RES		HOMER Pro	
	E_a/kWh	E_a/%	E_a/kWh	E_a/%
Base Case				
Load	1,116,896	43.3	1,116,900	42.1
Grid feed-in	1,462,122	56.7	1,538,909	57.9
Total	2,579,018	100	2,655,809	100
Scenario 1: Wind, Biomass & Grid				
Load	2,430,896	71.1	2,430,900	71.8
Grid feed-in	990,427	28.9	955,298	28.2
Total	3,421,323	100	3,386,198	100
Scenario 2: Wind, Biomass, PV & Grid				
Load	2,430,896	70.5	2,430,900	70.9
Grid feed-in	1,017,555	29.5	996,161	29.1
Total	3,448,450	100	3,427,061	100
Scenario 3: Wind, Biomass & BESS				
Load	2,178,677	100	2,082,043	100
Scenario 4: Wind, Biomass, PV & BESS				
Load	2,240,062	100	2,150,772	100
Scenario 5: Wind, PV & BESS				
Load	2,134,946	100	2,083,531	100
Scenario 6: Wind, PV & Grid				
Load	2,430,896	72.8	2,430,900	73
Grid feed-in	905,970	27.2	897,604	27
Total	3,336,866	100	3,328,504	100

Table 11: Primary site: Comparing the electricity generation from HY4RES with HOMER Pro.

	HY4RES		HOMER Pro	
	E_a/kWh	E_a/%	E_a/kWh	E_a/%
Base Case				
Wind	2,240,471	86.9	2,240,471	80.9
From grid	338.547	13.1	527,361	19.1
Total	2,579,018	100	2,767,833	100
Scenario 1: Wind, Biomass & Grid				
Wind	2,240,471	65.5	2,240,471	64.0
Biomass	219,000	6.4	219,000	6.3
From grid	961,323	28.1	1,038,751	29.7
Total	3,421,323	100	3,498,222	100
Scenario 2: Wind, Biomass, PV & Grid				
Wind	2,240,471	65	2,240,471	63.2
Biomass	219,000	6.4	219,000	6.2
PV	104,606	3	107,164	3
From grid	884,374	25.6	980,500	27.6
Total	3,448,450	100	3,547,135	100
Scenario 3: Wind, Biomass & BESS				
Wind	2,240,471	91.1	2,240,471	91.1
Biomass	219,000	8.9	218,974	8.9
Total	2,459,471	100	2,459,445	100
Scenario 4: Wind, Biomass, PV & BESS				
Wind	2,240,471	87.4	2,240,471	87.3
Biomass	219,000	8.5	218,950	8.5
PV	104,606	4.1	107,164	4.2
Total	2,564,077	100	2,566,585	100
Scenario 5: Wind, PV & BESS				
Wind	2,240,471	95.5	2,240,471	87.3
PV	104,606	4.5	107,164	4.2
Total	2,345,077	100	2,347,635	100
Scenario 6: Wind, PV & Grid				
Wind	2,240,471	67.1	2,240,471	65
PV	104,606	3.1	107,164	3.1
From grid	991,789	29.7	1,100,421	31.9
Total	3,336,866	100	3,448,057	100

Scenarios which only have a BESS and no grid access, are omitted in Table 12.

Table 12: Primary site: Comparing the cash-flows from feed-in and purchasing from the grid of HY4RES with HOMER Pro.

	HY4RES	HOMER Pro
Base Case		
Revenue / €	285,114	300,097
Expenses / €	128,919	200,819
Cash-flow / €	156,195	99,278
Scenario 1: Wind, Biomass & Grid		
Revenue / €	193,133	186,283
Expenses / €	366,273	395,556
Cash-flow / €	-173,140	-209,273
Scenario 2: Wind, Biomass, PV & Grid		
Revenue / €	198,423	194,251
Expenses / €	336,769	373,374
Cash-flow / €	-138,346	-179,123
Scenario 6: Wind, PV & Grid		
Revenue / €	176,664	175,033
Expenses / €	377,673	419,040
Cash-flow / €	-201,009	-244,007

3.1.2 Primary site: Base Case

With the input parameters from subsection 2.3, the electricity consumption by the load of the two processing facilities is displayed in Figure 7. As discussed before, it includes the consumption of Island Seafoods and Albatross Seafoods. It remains the same for the following primary site's simulations which do not include the biomass drying kiln. Table 10 displays the total electricity consumption by the loads and the amount sold to the grid as feed-in. Additionally, it compares theses values with the ones obtained from the HOMER Pro simulation.

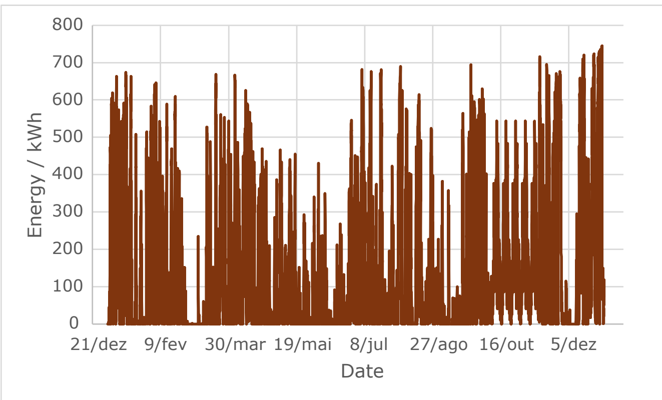

Figure 7: Primary site - Base case: electricity consumption throughout the year 2023.

In the base case, only the Vestas V52 wind turbine is operating as a generation asset. Its energy generation throughout the year can be seen in Figure 8. Table 11 holds the yearly total generation from wind and the electricity bought from the grid, also including percentage values to get a better understanding of the contribution of each.

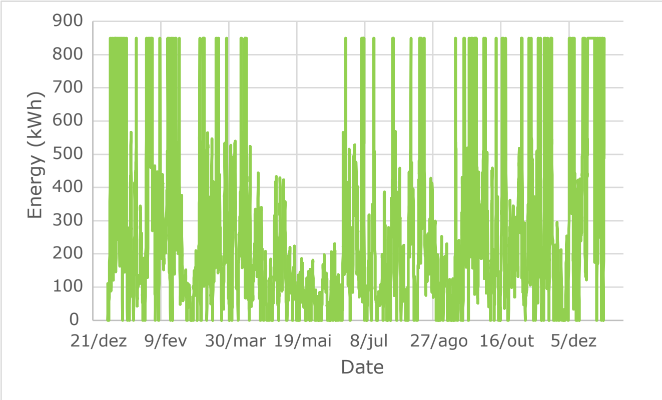

Figure 8: Primary site - Base case: electricity generation from the Vestas V52 wind turbine in 2023.

To get a better understanding of the times of the year when electricity has to be purchased from the grid or can be sold to the grid, the energy excess/deficit is plotted in Figure 9. As this is directly related to the electricity being sold to the grid and being bought from the grid, this data enables to compute the yearly cash-flows. Expenses from grid purchases as well as revenue from feed-in are compared in Table 12 with the values from HOMER Pro.

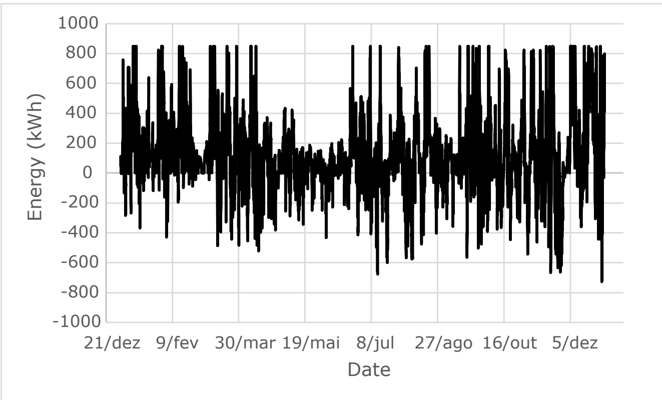

Figure 9: Primary site - Base case: Energy excess & deficit throughout the year 2023. Negative values express a deficit while positive ones represent excess.

In terms of system self-sufficiency, the HY4RES model reaches a value of 69.7 % in terms of hourly load directly supplied by the wind turbine generation. In Homer Pro this value is at 52.8 %.

3.1.3 Primary site: Wind, Biomass and Grid

This scenario extends the base case by adding the wood drying kiln and biomass generator. Hence, the additional consumption of the drying kiln is regarded as discussed in subsection 2.3. Figure 10 shows the new consumption profile with the biomass drying kiln. This profile is the same for all primary site's scenarios which include biomass and are connected to the grid. Table 10 compares the consumption and grid feed-in values from the two tools.

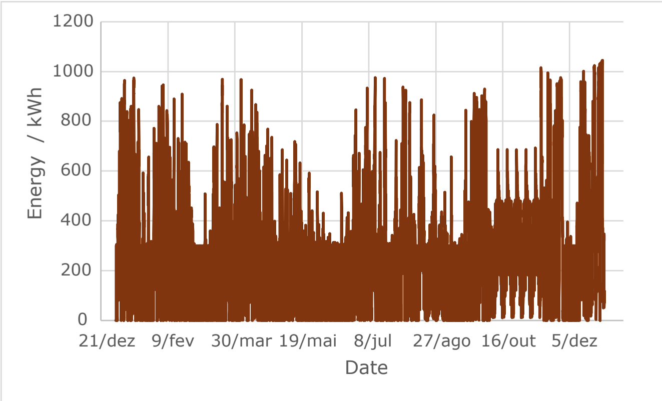

Figure 10: Primary site - Grid, Wind and Biomass: electricity consumption throughout the year 2023.

The generation profile depicted in Figure 11 includes the biomass generator which supports with 25 kW for 12 h of each day in addition to the Vestas V52 wind turbine.

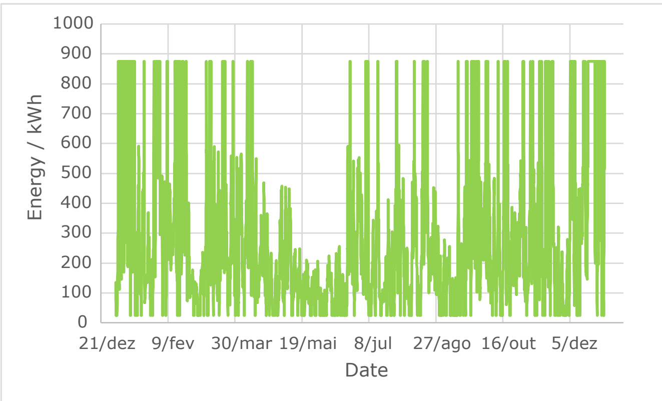

Figure 11: Primary site - Grid, Wind and Biomass: electricity generation in 2023.

This scenario reaches a self-sufficiency of 60.5 % and 57.3 % in HY4RES and HOMER Pro, correspondingly. Finally, the energy balance is depicted in Figure 12.

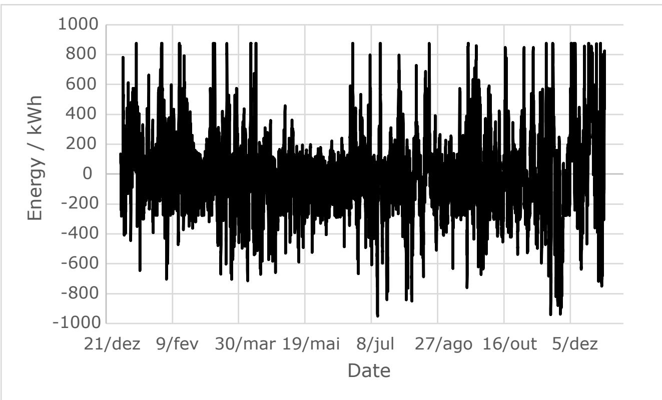

Figure 12: Primary site - Grid, Wind and Biomass: Energy excess & deficit throughout the year 2023. Negative values express a deficit while positive ones represent excess.

3.1.4 Primary site: Wind, biomass, PV and grid

This scenario includes the rooftop PV system on the processing facilities' roofs of 120 kW_p. The consumption profile remains the same as shown in the biomass scenario before, only the generation profile is altered by the PV generation. It is shown in Figure 13.

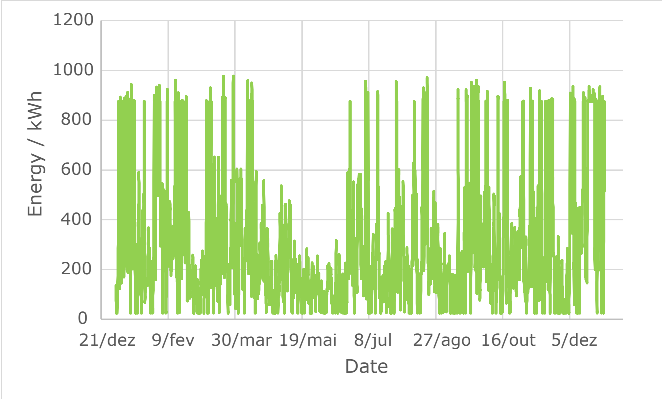

Figure 13: Primary site - Grid, Wind, Biomass and PV: electricity generation in 2023.

The individual PV generation profile is depicted in Figure 14.

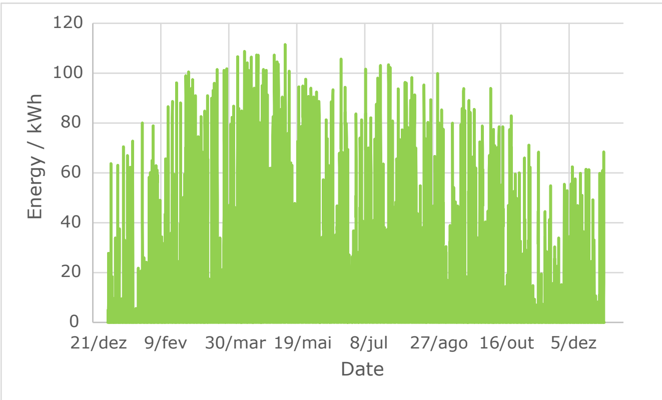

Figure 14: PV electricity generation profile for 2023.

Furthermore, a slight change in the energy balance can be observed in Figure 15. As a comparison, Figure 16 shows the contribution of each generation technology as well as the load served each hour of the year from the HOMER Pro simulation. This scenario reaches a self-sufficiency of 63.6 % and 59.7 % in HY4RES and HOMER Pro, correspondingly.

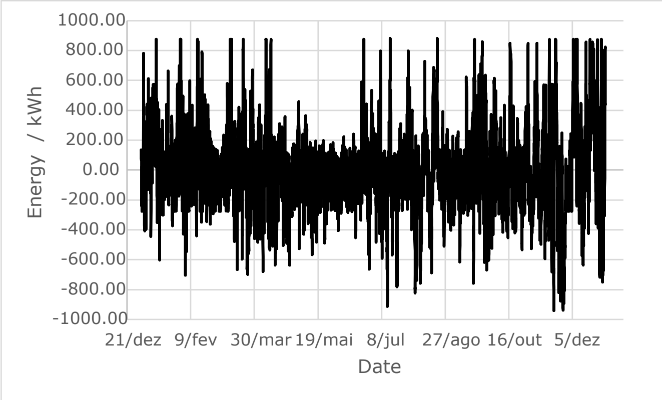

Figure 15: Primary site - Grid, Wind, Biomass and PV: Energy excess & deficit throughout the year 2023. Negative values express a deficit while positive ones represent excess.

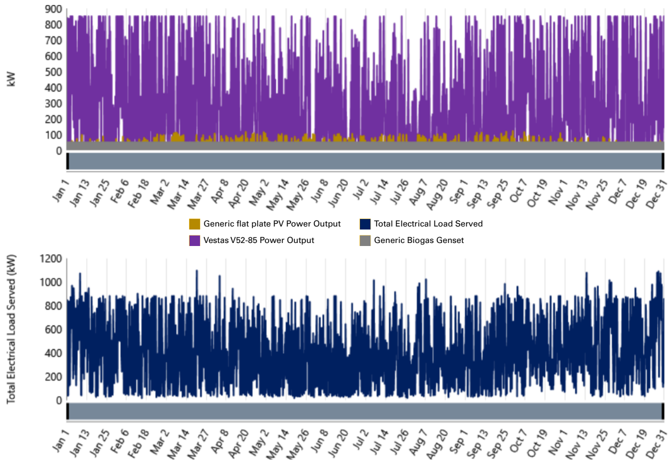

Figure 16: Primary site - Grid, Wind, Biomass and PV: hourly generation profile (upper graph) of each generating technology and the hourly loads (lower graph) served in HOMER Pro. From [14].

3.1.5 Primary site: Wind, biomass and BESS

This scenario does not have access to the grid, energy balancing is fully done by the BESS. Due to the same electricity consumption, the hourly profile for this scenario is the same as shown in Figure 10. However, due to the limited capacity of the BESS, the demand can not be met at every hour of the year, creating a deficit. This is at 10.4 % and 14 % [14] in the HY4RES and HOMER Pro simulation, respectively. This leads to a reduction in available electricity for the wood drying kiln. In HY4RES, the residual electricity available for wood drying amounts to 1,061,781 kWh, which translates to 531 t of dried wood per year instead of 657 t in the grid tied scenarios — a capacity reduction of 19 %. HOMER Pro on the other hand, simulated with a capacity shortage of 20 % and resulted in 483 t of dried wood per year. This development being related to the system only relying on the BESS, it is of interest to observe its performance. The hourly SOC evolution of the 22 MWh BESS is shown in Figure 17. With the corresponding hourly generation data being summarized in Table 11. In the HY4RES and HOMER Pro the annual energy being charged to the BESS is 709,138 kWh and 776,419 kWh [14], respectively.

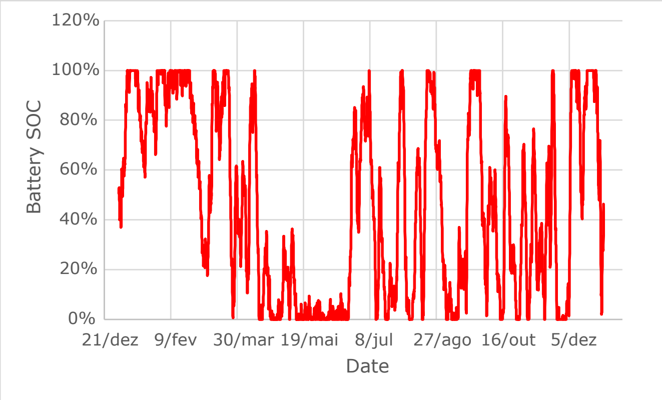

Figure 17: Primary site - Wind, Biomass and BESS: hourly SOC variation of the BESS in 2023.

3.1.6 Primary site: Wind, biomass, BESS and PV

Like the previous system, this system is also off-grid. By the addition of solar PV, the annual energy deficit was reduced to 7.9 %, a reduction of 24 % in unmet electricity demand compared with the previous scenario. The simulation in HOMER Pro achieved a reduction of 30 %. As a result of the electricity deficit, the operation of the wood drying kiln has to be adjusted. In the HY4RES model, this leads to a remaining capacity of 562 t of wood being dried per year, a capacity reduction of 15 % compared with the 657 t under the grid tied scenario. The corresponding consumption and generation summaries are found in Table 10 and Table 11, respectively. The electricity being charged by the BESS decreases slightly compared to the previous scenario to 693,667 kWh.

3.1.7 Primary site: Wind, PV and BESS

To sustain the same level of unmet electricity demand, the capacity of the wood drying kiln is reduced to 562 t per year as shown in the previous scenario. As the biomass generator does not operate, the dried wood is sold instead of being used directly at the facility. HOMER Pro is able to sustain its energy deficit while increasing the number of BESS to a total capacity of 63 MWh. The HY4RES model is not able to fully supply the reduced hourly loads and as a result, the deficit increases further by 4.7 %. As a result, only 509 t of wood can be dried annually. Due to the larger BESS, the SOC shows a different trend, as depicted in Figure 18.

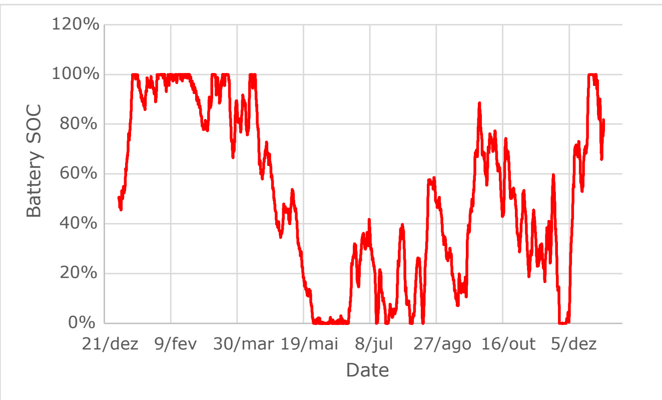

Figure 18: Primary site - Wind, PV and BESS: hourly SOC variation of the BESS in 2023.

3.1.8 Primary site: Wind, PV and grid

As with the previous scenarios, the generation, consumption and cash-flow results are presented in Table 11, Table 10 and Table 12, respectively. Additionally, the energy excess/deficit — in other words, the energy being drawn from the grid or sold to the grid — is depicted in Figure 19.

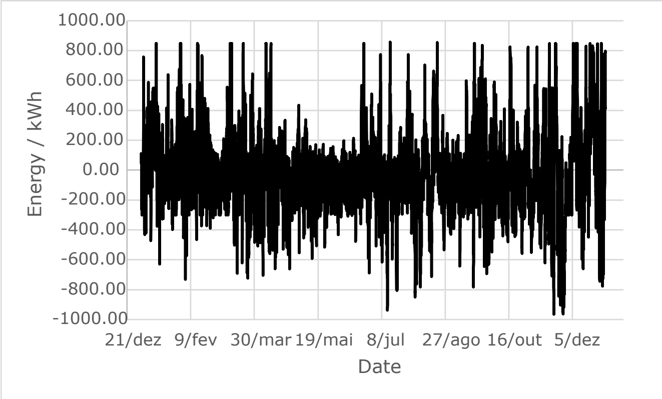

Figure 19: Primary site - Wind, PV and grid: Energy excess & deficit throughout the year 2023. Negative values express a deficit while positive ones represent excess.

The revenue from electricity sold to the grid and expenses from purchasing electricity from the grid are compared in Figure 20. This scenario reaches a self-sufficiency of 59.2 % and 54.7 % in HY4RES and HOMER Pro, correspondingly.

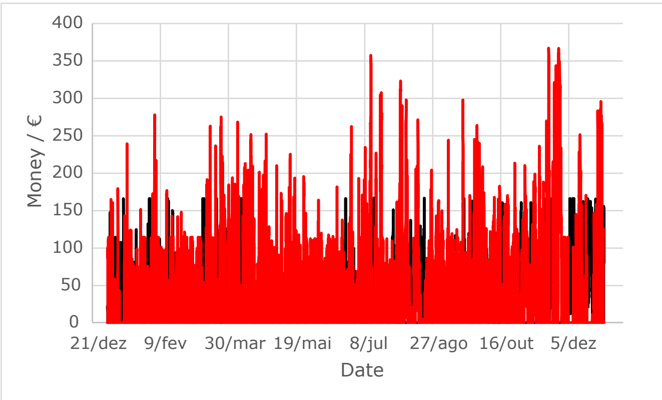

Figure 20: Primary site - Wind, PV and grid: Expenses (red) and income (black) throughout the year 2023.

3.1.9 Secondary site

This section compiles the results for the secondary site in terms of energy consumption, generation and cash-flow in Table 13, Table 14 and Table 15, respectively. All scenarios' results are summarized in the tables below, while the following sections present extended results for each individual scenario.

Table 13: Secondary site: Comparing the electricity consumption values from HY4RES with HOMER Pro.

	HY4RES		HOMER Pro	
	E_a/kWh	E_a/%	E_a/kWh	E_a/%
Base Case				
Load	438,000	41.3	438,000	48.6
Grid feed-in	623,071	58.7	462.325	51.4
Total	1,061,071	100	900,325	100
Scenario 1: Hydropower, PV & Grid				
Load	438,000	39	438,000	45.4
Grid feed-in	684,858	61	526,993	54.6
Total	1,122,858	100	964,993	100
Scenario 2: Hydropower, PV & BESS				
Load	328,824	100	387,829	100

Table 14: Secondary site: Comparing the electricity generation from HY4RES with HOMER Pro.

	HY4RES		HOMER Pro	
	E_a/kWh	E_a/%	E_a/kWh	E_a/%
Base Case				
SHP	884,225	83.3	809,410	89.9
From grid	176,850	16.7	90,915	10.1
Total	1,061,075	100	900,325	100
Scenario 1: Hydropower, PV & grid				
SHP	884,225	78.7	809,410	83.4
PV	104,606	9.3	107,164	11
From grid	134,031	11.9	54,110	5.6
Total	1,122,862	100	970,684	100
Scenario 2: Hydropower, PV & BESS				
SHP	884,225	89.4	809,410	88.3
PV	104,606	10.6	107,164	11.7
Total	988,831	100	916,574	100

Scenarios which only have a BESS and no grid access, are omitted in Table 15.

Table 15: Secondary site: Comparing the cash-flows from feed-in and purchasing from the grid of HY4RES with HOMER Pro.

	HY4RES	HOMER Pro
Base Case		
Revenue / €	121,499	90,153
Expenses / €	67,344	34,620
Cash-flow / €	54,154	55,532
Scenario 1: Hydropower, PV & grid		
Revenue / €	133,547	102,764
Expenses / €	51,039	20,605
Cash-flow / €	82,508	82,159

3.1.10 Secondary site: Base Case

The hydropower generation is depicted in Figure 21.

Figure 21: Secondary site - Base case: electricity generation from the SHP in 2023.

This scenario reaches a self-sufficiency of 59.6 % and 79.2 % in HY4RES and HOMER Pro, correspondingly. Finally, the energy deficit/excess is plotted in Figure 22.

Figure 22: Secondary site - Base case: Energy excess & deficit throughout the year 2023. Negative values express a deficit while positive ones represent excess.

3.1.11 Secondary site: Hydropower, PV and Grid

This scenario reaches a self-sufficiency of 69.4 % and 87.6 % in HY4RES and HOMER Pro, correspondingly. The renewables' hourly generation profile is found in Figure 23.

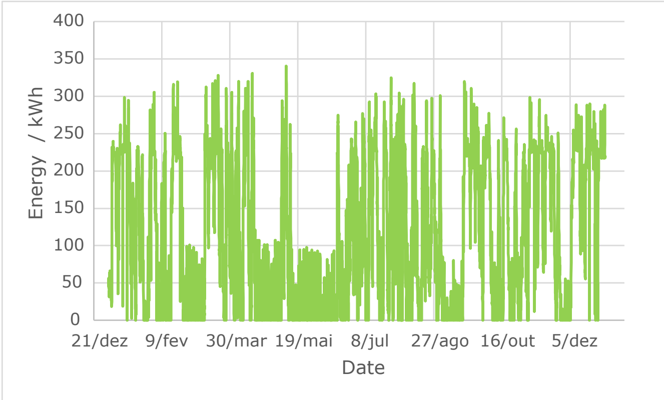

Figure 23: Secondary site - Hydropower, PV and Grid: electricity generation in 2023.

As a comparison, the hydropower and PV output, as well as the grid purchases from the HOMER Pro simulation are depicted in Figure 24.

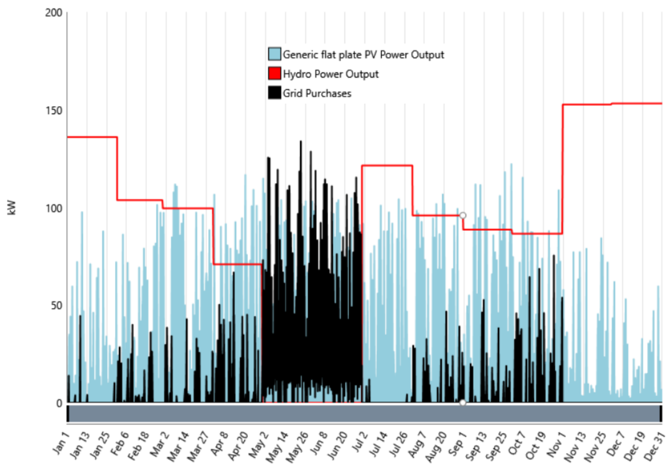

Figure 24: Secondary site - Hydropower, PV and Grid: hourly generation profiles from HOMER Pro. From [14].

3.1.12 Secondary site: Hydropower, PV and BESS

The simulation in HOMER Pro results in 11.5 % of the original load of the WWTP to be unmet. In HY4RES, this percentage lies at 24.9 %. In case of the BESS, a usable capacity of the BESS of 320 kWh is used in HOMER Pro. The BESS is charged with 25,055 kWh and 13,123 kWh per year in HY4RES and HOMER Pro, respectively. The evolution of the battery's SOC can be seen in Figure 25.

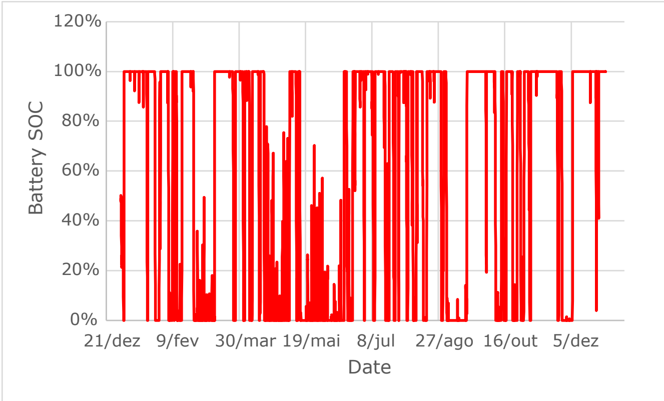

Figure 25: Secondary site - Hydropower, PV and BESS: hourly SOC variation of the 400 kWh BESS in 2023.

3.2 HY4RES V2

3.2.1 Optimal system primary site

Optimizing the primary system with the Evolutionary method in Solver, leads to a global optimum of an NPV = 957.85 € with a PV installed power of 8 kW_p and no BESS or BG. The remaining results for this site's optimal scenario are presented in Table 17. In order to observe the improvement from the baseline to the optimal scenario, the baseline's results are also included in Table 17. The fixed consumption profile does not change visibly compared to the combined site, due to the low contribution of the WWTP. Hence, it is only printed once in Figure 35 for the combined site. The consumption of the flexible load for this specific case is presented in Figure 26.

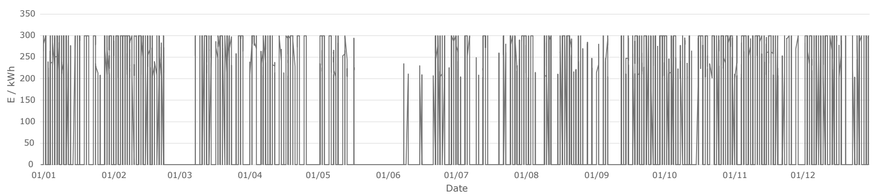

Figure 26: Wood drying kiln load profile for the primary site, simulated with HY4RES V2.

The contribution of each renewable energy technology to the total generation on site are summarized in the pie chart in Figure 27. Additionally, Figure 28 and Figure 29 depict the hourly generation profile of the Vestas V52 and the PV system, respectively.

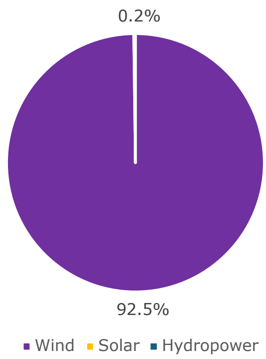

Figure 27: Contribution of each renewable energy technology to the annual site's generation for the primary site, simulated with HY4RES V2. 100 % corresponds to the total generation plus the electricity purchased from the grid.

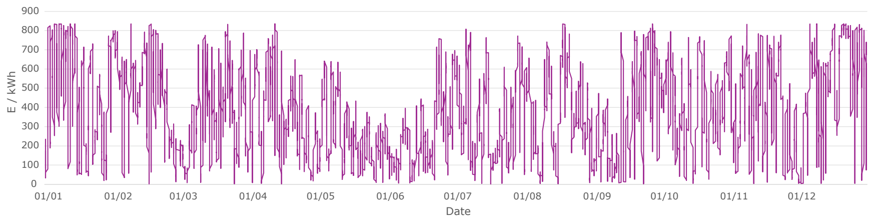

Figure 28: Vestas V52 generation profile for the primary site, simulated with HY4RES V2.

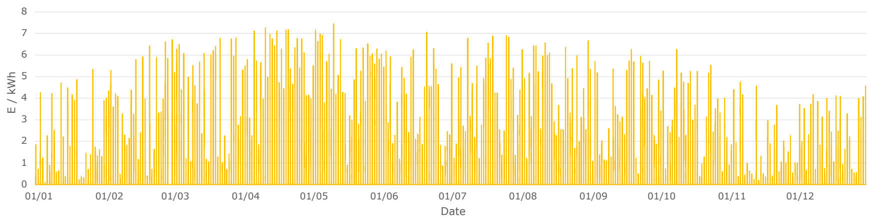

Figure 29: PV generation profile for the primary site, simulated with HY4RES V2.

The results from the financial simulation are found in Figure 30 and Figure 31 which show the annual DCF and the cumulative DCF along the project's lifetime, respectively.

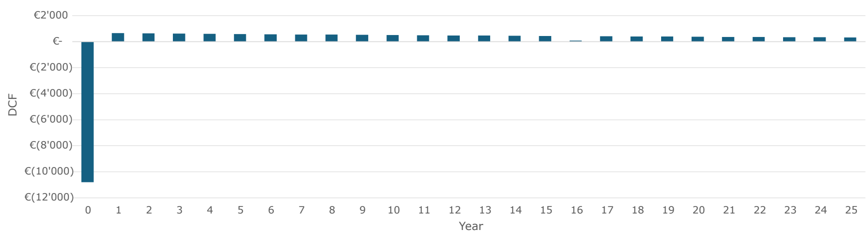

Figure 30: DCF for the primary site, simulated with HY4RES V2.

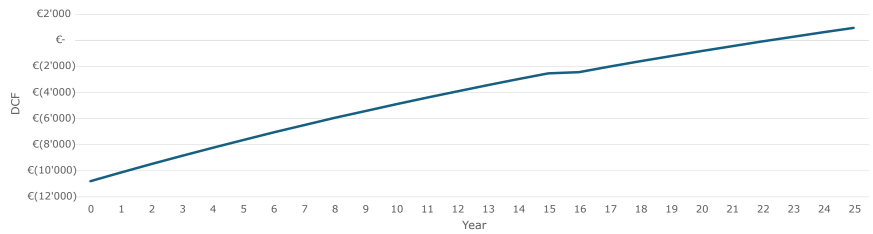

Figure 31: Cumulative DCF for the primary site, simulated with HY4RES V2.

Finally, the results from the sensitivity analysis are presented in Table 16. As the optimal system does not include a BG, it is decided to omit the sensitivity analysis of the BG conversion efficiency η_{BG}.

Table 16: Results from the sensitivity analysis.

Parameters	Sensitivity	NPV / €	PP / years
r	+10 %	234	25.19
r	−10 %	1,754	21.64
I_{PV}	+10 %	-396	> 25
I_{PV}	−10 %	2312	19.64
$p_{\mathrm{grid,sell}}$	+10 %	1465	21.99
$p_{\mathrm{grid,sell}}$	−10 %	451	24.61
$p_{\mathrm{grid,buy}}$	+10 %	1748	21.37
$p_{\mathrm{grid,buy}}$	−10 %	168	25.46

3.2.2 Optimal system secondary site

The secondary site does not have the grid injection limit compared to the two other sites. Additionally, the SHP has a fixed PPA contract at the price displayed in Table 7. Still, the Evolutionary or GRG non-linear were not able to find a feasible solution that includes an investment in any of the three technologies — PV, BESS and BG. Hence, the baseline is considered the optimal system. Its key performance metrics are again displayed in Table 17. Figure 32 displays the consumption profile of the WWTP, while Figure 33 displays the SHP generation profile. Finally, Figure 34 presents the energy balance with the power grid.

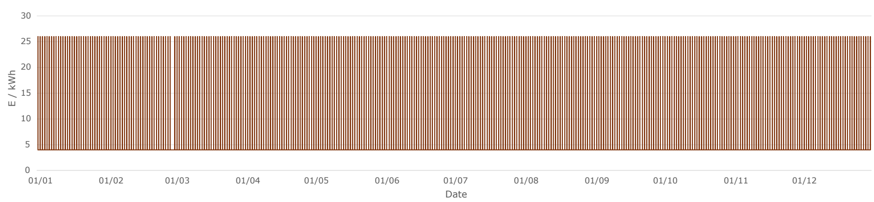

Figure 32: WWTP load profile for the secondary site, simulated with HY4RES V2.

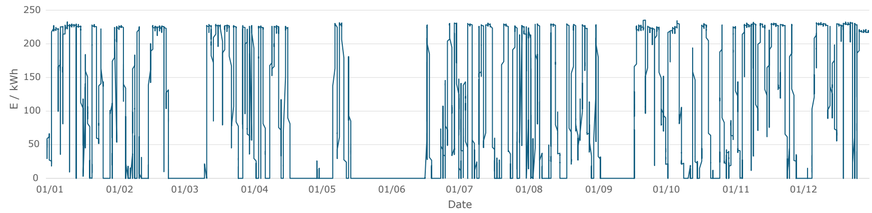

Figure 33: SHP generation profile for the secondary site, simulated with HY4RES V2.

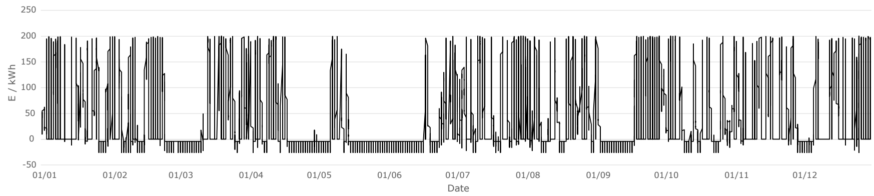

Figure 34: Grid balance for the secondary site, simulated with HY4RES V2. Positive values correspond to an excess which is sold to the grid while negative ones are a deficit and must be bought from the grid.

3.2.3 Optimal system combined site

When the grid injection limit of 120 kW is active, no optimization of the system is possible. Any addition of a PV system, BESS or BG directly leads to a negative NPV. It can therefore be concluded that the combined system is well balanced in terms of generation and consumption, the latter of which is strongly supported by the demand side flexibility of the wood drying kiln. The best evidence of this is the SSR which lies at 94 % and an SCR of 84 %. Other key outcomes are presented in Table 17. Figure 35 shows the hourly consumption profile of the combined fixed loads which include the WWTP and the two seafood processing plants. Figure 36 displays the hourly load profile of the flexible load — the wood drying kiln.

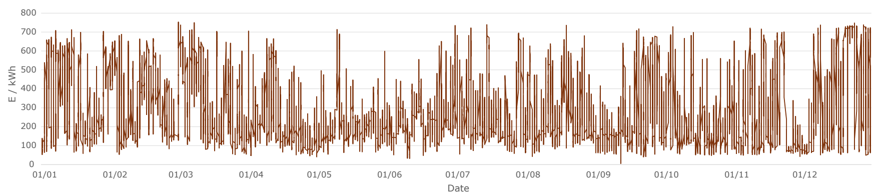

Figure 35: Fixed load profile for the combined site, simulated with HY4RES V2.

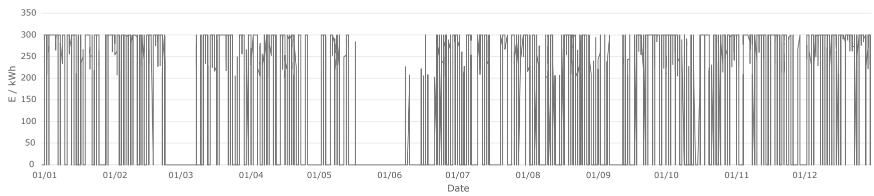

Figure 36: Wood drying kiln load profile for the combined site, simulated with HY4RES V2.

The grid balance, between the system's energy deficit/excess, is shown in Figure 37. Additionally, the contribution of each renewable energy technology to the total generation on site are summarized in the pie chart in Figure 38. The hourly wind generation profile is the same as for the primary site and hence only depicted once in Figure 28. The same applies for the SHP generation profile of the secondary site, depicted in Figure 33.

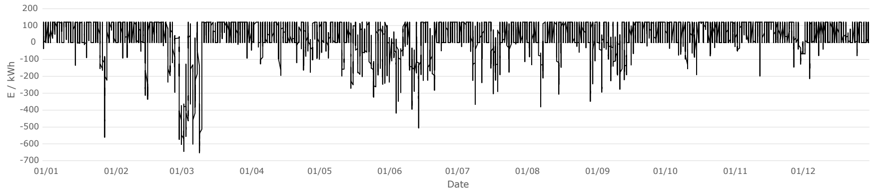

Figure 37: Grid balance for the combined site, simulated with HY4RES V2. Positive values correspond to an excess which is sold to the grid while negative ones are a deficit and must be bought from the grid.

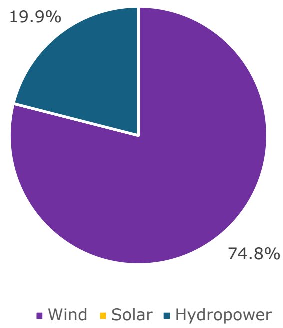

Figure 38: Contribution of each renewable energy technology to the annual site's generation for the combined site, simulated with HY4RES V2. 100 % corresponds to the total generation plus the electricity purchased from the grid.

3.2.4 Optimal system combined site SSR

This system takes the combined site but instead of optimizing it for the highest NPV, it is optimized for the highest SSR. With an installation of 101 kW PV, 109 kWh of BESS and 247 kW BG, a self-sufficiency of 99 % is reached. The remaining results are shown in Table 17. Figure 39 displays the contribution of each renewable energy technology to the total consumption on site.

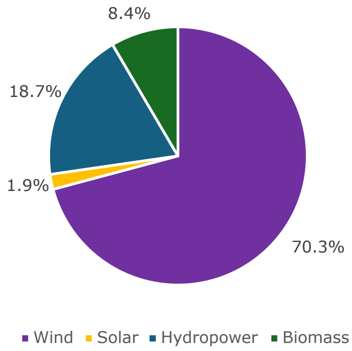

Figure 39: Contribution of each renewable energy technology to the annual site's generation for the combined site SSR, simulated with HY4RES V2. 100 % corresponds to the total generation plus the electricity purchased from the grid.

The PV and BG generation profiles are found in Figure 40 and Figure 41, respectively. Figure 42 shows the development of the SOC of the BESS. Finally, Figure 43 depicts the cumulative dried wood available.

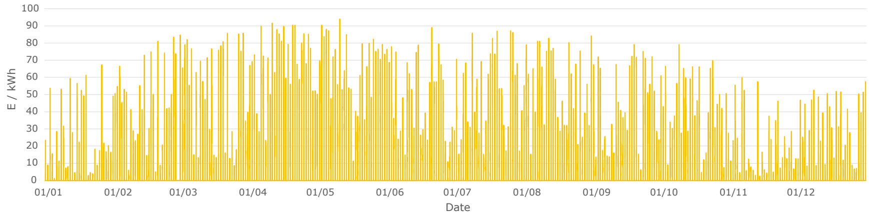

Figure 40: PV generation profile for the combined site SSR, simulated with HY4RES V2.

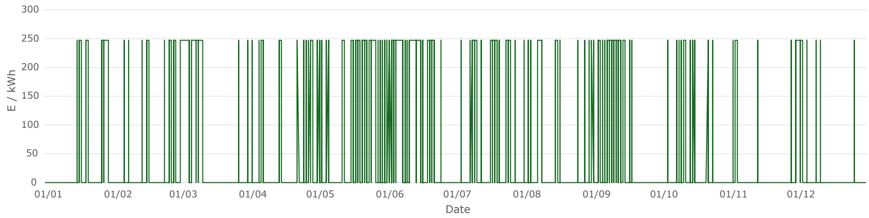

Figure 41: BG generation profile for the combined site SSR, simulated with HY4RES V2.

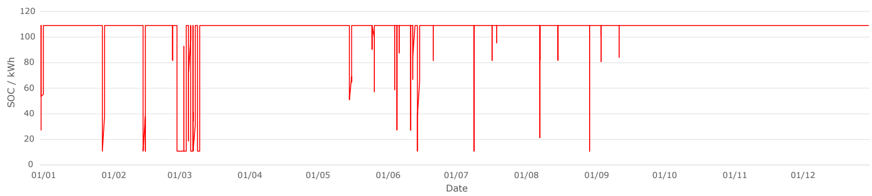

Figure 42: BESS SOC profile for the combined site SSR, simulated with HY4RES V2.

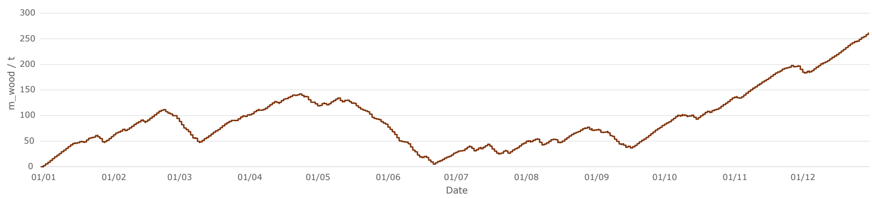

Figure 43: Cumulative available dried wood for the combined site SSR, simulated with HY4RES V2.

3.2.5 Site comparison

As a comparative analysis, the optimal systems' results for the primary, secondary and combined system are displayed in Table 17.

Table 17: Comparison of optimal system results for the primary, secondary and combined site using HY4RES V2. For the secondary and combined site, only the optimal system's results are given as no optimization of the given system was possible.

	$P_{optimal}$	$P_{baseline}$	$S_{optimal}$	$C_{optimal}$	C_{SSR}
P_{PV} / kW	8	0	0	0	101
P_{BG} / kW	0	0	0	0	247
C_{BESS} / kWh	0	0	0	0	109
SSR / %	92	91	94	94	99
SCR / %	85	85	64	84	80
$E_{a,from\,grid}$ / kWh	261,368	263,519	34,852	262,613	33,615
$E_{a,to\,grid}$ / kWh	421,706	420,323	315,111	481,768	642,316
$E_{a,BESS-ch}$ / kWh	0	0	0	0	2,078
$E_{a,BESS-dis}$ / kWh	0	0	0	0	1,798
$n_{a,BESS-cycles}$	0	0	0	0	18
NPV / €	957.85	-	-	-	$-4,562,928$
PP / years	23.22	-	-	-	> 25
MIRR / %	6 %	-	-	-	-
I_{tot} / €	11,669	0	0	0	1,778,637
PI	0.08	-	-	-	-
$LCOE_{PV}$ / $\frac{€}{MWh}$	228.3	0	0	0	237.3
$LCOE_{BG}$ / $\frac{€}{MWh}$	0	0	0	0	1,930.6
Grid cash-flow / €	32,179	31,336	22,003	49,555	124,008
Loss (grid injection limit) / €	17,502	17,376	0	41,017	288,694
$m_{wood,dried}$ / t	369.06	367.61	0	656.84	261.12
$m_{CO_2-eq.}$ / t	48.9	49.28	6.52	43.5	33.62

P Primary site, **S** Secondary site, **C** Combined site, C_{SSR} optimized for SSR

4 Discussion

4.1 Comparison with HOMER Pro

4.1.1 Primary site: Base Case

The variability of the electric loads throughout the year becomes evident in Figure 7, where the load fluctuates and reaches it's peak, slightly above 700 kW in December 2023. This aligns with the 720 kW from HOMER Pro, which were approximately the highest loads, supplied by the wind turbine in the simulation [14]. As the same hourly consumption data for 2023 is used for HOMER Pro and the HY4RES tool, the yearly energy consumption is almost the same for both simulation tools, as seen in Table 10. The slight deviation can be explained by rounding differences of the values added.

On the generation side, the yearly total energy generated by the wind turbine is the same for both models. However, comparing the hourly generation profiles in Figure 11 and Figure 16, it becomes evident that there are some discrepancies. The HOMER Pro simulation results in a more homogeneous output power throughout the year, showing the typical dip in summer but remaining stable. The HY4RES simulation on the other hand does show a strong decrease in generation during May. This deviation in wind power output profile can be explained by the underlying wind speeds used for simulation. HOMER Pro utilizes 30 years mean hourly wind speeds as discussed in subsection 2.3, while HY4RES in this specific case uses wind speeds only from the year 2023. The latter gives stronger emphasis to specific events, or wind speeds that only occurred in 2023, while the former reduces the effect of such events due to using the mean hourly wind speeds over a 30 year period. However, the HY4RES model's wind simulation aligns better with the hourly load profile, leading to a reduction in grid-feed in but also a reduction in electricity from the grid. This becomes evident when comparing the cash-flows in Table 12. HY4RES predicts a much higher positive cash-flow compared to HOMER Pro, once again confirming that the input parameters have the largest impact on the results. The higher degree of energy excess in HY4RES is emphasized in Figure 9, here the positive values outweigh the negative ones. This leads to a higher degree of self-sufficiency in the HY4RES model.

4.1.2 Primary site: Wind, biomass and grid

Comparing this scenario's load profile in Figure 10 with the base case in Figure 7, the additional load of the wood drying kiln becomes evident. It increases the maximum power demand close to and slightly above 1000 kW. However, when comparing the two models, it becomes evident that the load profiles show a different evolution over time, as seen in Figure 16 and Figure 10. The results in Table 10, show a strong alignment of the two models. On the generation side, Table 11 confirms this. However, the discrepancies discussed for the Base Case, are reduced by the implementation of the BG and additional load of the wood drying kiln. This also leads to the cash-flows to only show slight deviations from HOMER Pro to HY4RES, as shown in Table 12. It is important to notice at this point that the negative resulting cash-flow for both models originates in the distribution of the annual excess electricity from the Base Case to the hourly loads of the wood drying kiln. Hence, the negative cash-flows should not be misinterpreted. For a more detailed simulation, it is recommended to adjust the load of the wood drying kiln only to the hours of the year where an excess of electricity is present and only to the capacity of the power available at that specific hour. This would reduce the resulting cash-flow. Additionally, it is worth noting that the cash-flow presented only accounts for trading electricity with the power grid, not the business of the dried wood which would have to be included for a more holistic view. This discussion also applies for the following scenarios which include the biomass drying kiln. As a consequence of this load, the energy balance is much more balanced in terms of grid injection/supply, as can be seen in Figure 10. Due to the misalignment of the kiln with the excess electricity, the self-sufficiency of the system decreases, even though it should increase, if managed correctly. This is the case both for HOMER Pro and HY4RES. The difference between both models is now only 3.2 %, compared to the 16.9 % for the Base Case. The closer alignment can be lead back to the input data and distribution of the drying kiln's load profile which is slightly different than the one applied in HOMER Pro. The BG has a limited effect on the results, as the generation profile is constant with 25 kW each hour of the year for both models. This constant profile can be seen in Figure 16 for the HOMER Pro simulation.

4.1.3 Primary site: Wind, biomass, PV and grid

On the load side, both simulations result in similar values, as displayed in Table 10. Only the grid feed-in differs slightly which can be explained by the differing hourly generation profiles. Comparing the annual electricity generation for both models in Table 11, they align well, only showing slight deviations. The annual electricity generation of the solar PV system is lower by 2,558 kWh in HY4RES compared to HOMER Pro. The hourly generation profile is found in Figure 14 and follows the typical trend of a peak in the summer months and lower production during winter. Thanks to the PV system, the self-sufficiency of the system could be increased by 3.1 % and 2.4 % compared to the previous scenario in HY4RES and HOMER Pro, respectively.

4.1.4 Primary site: Wind, biomass and BESS

In HY4RES the sum of the hourly loads that can still be supplied over the course of the year is 96,634 kWh higher compared to the one in HOMER Pro. HY4RES uses a simplified BESS model which disregards losses and simply uses the nominal capacity, instead of the useful capacity which is considered in HOMER Pro. Hence, the simulation in HOMER Pro results in a lower consumption, as shown in Table 10. This is confirmed by the electricity deficit which is 3.6 % higher in HOMER Pro than in HY4RES. As a result, the biomass drying kiln can be operated at a higher capacity in the HY4RES model and leads to an additional 48 t of dried wood per year. The dip in wind turbine generation in May, as shown in Figure 8, directly affects the SOC of the BESS during that same period. Figure 17 shows that there is not enough excess electricity to recharge the BESS during this period. On the generation side, the annual values align very well for both models as presented in Table 11.

4.1.5 Primary site: Wind, biomass, BESS and PV

As with the previous scenario, the annual generation align very well for both models. This is also true for the contribution of each technology to the grand total. Both becomes evident when observing the values in Table 11. From Table 10 one can observe the impact of the simplified BESS model in HY4RES, as discussed for the previous scenario. In terms of unmet electricity demand, HY4RES is able to supply 6 % more compared with HOMER Pro, also influenced by the aforementioned battery modeling.

However, the addition of the rooftop PV system increases the wood drying capacity by 6 % in the HY4RES model. It is however unclear why the electricity charged in the BESS decreases slightly by 15,471 kWh from the previous scenario to this scenario, the only difference being the implementation of solar PV. The amendment of the system should lead to more electricity being available for charging the BESS, not less.

4.1.6 Primary site: Wind, PV and BESS

With same wood drying capacity which resulted from the previous scenario, HY4RES was not able to meet its all of the hourly demand. HOMER Pro did succeed in this, while the former still has an additional 4.7 % of electricity demand unmet. It is likely that this difference originates from the wood drying capacity in HY4RES being met by Scenario 4. This difference is apparent as well in Table 11. The generation side is well aligned as presented in Table 11. On the topics of storage, the SOC in Figure 18 of the 63 MWh BESS is a lot less volatile compared to the smaller one in Figure 17. In HOMER Pro, this scenario was regarded as the worst one in terms of cost and technical feasibility. With the size of the BESS in mind, this can only be underlined.

4.1.7 Primary site: Wind, PV and grid

In terms of loads, Table 10 shows the alignment of both models. Likewise the generation data only shows slight deviations in electricity being drawn from the grid in Table 11. In terms of cash-flows, the higher demand for grid electricity in HOMER Pro leads to higher expenses in Table 12. Overall, the expenses dominate the income also in the HY4RES model, as depicted in Figure 20. The rate of self-sufficiency differs by 4.5 % between the models. In the HY4RES model, it is 1.3 % lower compared to Scenario 1 which includes BG instead of the PV system.

4.1.8 Secondary site: Base Case

As the total daily load of the WWTP is the same in HOMER Pro and HY4RES, the yearly total is the same for both. This becomes evident when consulting Table 13. However, due to the fixed hourly load in HY4RES, different grid feed-in and grid electricity can be registered than for HOMER Pro. Also, the metered annual generation of the SHP is higher by 8.5 % than the one simulated in HOMER Pro. This also adds to the differences in electricity exchanged with the grid. Figure 21 shows the hydropower generation profile in HY4RES while Figure 24 depicts the one in HOMER Pro. The latter uses a simplified simulation approach where the hourly generation only varies between months, but not between hours within a month. Additionally, it assumes higher flow rates during the winter, leading to a higher power output for these months and a lower one during summer. The metered hydropower generation data in Figure 21, does correctly show the hourly variation and does show the strong seasonal pattern. These two simplifications in the HOMER Pro simulation lead to a lower annual generation as mentioned above. In terms of cash-flows, the resulting cash-flow only shows a deviation of 2.5 %, as displayed in Table 15. The revenue and expenses do differ from one model to the other. However, this can be traced back to the different grid electricity exchange mentioned above.

4.1.9 Secondary site: Hydropower, PV and grid

The extension of the system by the rooftop PV system results in a higher grid injection and lower grid dependency as expected. This is confirmed by both models with the values shown in Table 13 and Table 14. For HOMER Pro, it becomes evident from Figure 24 how the grid purchases dominate during the period where hydropower output is close to zero, while remaining low during the rest of the year. Additionally, the generation from the PV system becomes evident when comparing Figure 21 with Figure 23. As in the Base Case, the resulting cash-flows are quite similar for both models in Table 15, while revenue and expenses differ again due to a difference in electricity exchanged with the grid.

4.1.10 Secondary site: Hydropower, PV and BESS

Due to the fixed hourly load of the WWTP in HY4RES, it results in an additional 13.4 % of electricity demand unmet compared to HOMER Pro. This is also evident when comparing the values from Scenario 1 and Scenario 2 in Table 13. Additionally, simplified simulation of the BESS in HY4RES results in 48 % more electricity being charged in the battery. Figure 25 shows the operation of the BESS throughout the year. The SOC is stable at 100 % during several periods of the year which indicates over sizing of the BESS. Likewise, there are a few periods when renewables' generation is not sufficient to supply the loads or charge the battery, these are the periods when a deficit occurs.

4.2 HY4RES V2

4.2.1 Optimal system primary site

The results show that the Vestas V52 wind turbine is over sized. At a self-sufficiency of 91 % for the baseline and an annual energy sold to the grid of 420,323 kWh, despite the grid injection limit, the system does not leave much room for improvement. The Evolutionary method of Solver still found a global optimum for the NPV at 957.85 € with a PV installed power of 8 kW. This addition only improves system performance slightly compared to the baseline as evident in Table 17, contributing only 0.2 % of generation as shown in Figure 27. SSR rises by 1 % while SCR remains stable at 85 %. Emission reductions below 1 % were achieved while the monetary losses from the grid injection limit rise by 126 €per year.

The system's cumulative DCF in Figure 31 show the increasing cumulative values from the initial investment of 11,669 €. The curve turns horizontal in year 16 when a new PV converter is purchased and installed. The total monetary losses due to the grid injection limit sum to 17, 502 € annually. With a PP of 23.22 years it is below the project lifetime of 25 years but much higher than the average for residential rooftop PV projects which lies at 10 years [41]. It is decided to compare it to the average for residential installations in Ireland compared to Commercial & Industrial (C&I) as the size of 8 kW corresponds to the former. As the PP is a financial metric defined by management, it is up to the company to decided whether this PP is acceptable or not. The LCOE is within the range of rooftop solar projects for residential clients in the US, which lies between $138-321\ \frac{€}{\mathrm{MWh}}$ [42]. As no accurate data is available for Ireland, these values are used for comparative reasons. The low financial viability is also expressed by the MIRR which almost equals the discount rate at 6 %.

In terms of NPV, the positive value of 957.85 € suggests a viable project. However, as it is only slightly above zero, it is decided to conduct a sensitivity analysis on the most important parameters to ensure the reliability of the indicator. The discount rate r has a strong influence on the NPV, a 10 % increase in r leads to a 76 % decrease in NPV, while a 10 % decrease in r leads to a 45 % increase. The effect of the discount rate on the PP is smaller. However, for an increase or decrease the NPV remains positive. The strongest influence has the sensitivity in investment cost. In case of a 10 % increase, it would tip the NPV to be negative and hence render the project non-viable in terms of this financial indicator. For a 10 % decrease in investment costs, an increase of 59 % in NPV is achieved while the PP can be decreased to 19.64 years. This emphasizes the importance of investment cost as the positive DCF are small each year, as evident from Figure 30. The influence of the sensitivity on the electricity purchase price and feed-in tariff is similar. The ones from selling electricity to the grid having a lower impact on NPV and PP due to the grid injection limit. The sensitivity on the purchase price being larger, it is important to highlight its development in case of a 10 % decrease in purchase price which leads to an NPV of 168 € or a 82 % reduction. This is the lowest positive NPV of the analysis while showing the highest PP of 25.46 years. Especially as some of the parameters are driving the NPV close to zero, a Monte Carlo simulation is recommended to observe the added sensitivity of the parameters and the probability of the NPV staying positive.

4.2.2 Optimal system secondary site

In case of the secondary site, the SHP has a much higher generation capacity than the peak load of the WWTP, 250 kW compared to 26 kW. An energy deficit is only present during the months where the SHP generation is zero. This is the case for March, June and parts of September as seen in Figure 34. This combination leads to an SSR of 94 % and an SCR of 64 %. The latter of which originates from the high grid feed-in compared to the electricity purchase at 315,111 kWh and 34,852 kWh, respectively. Even though the system does not have a grid injection limit, the annual grid cash-flow results in 22,003 €due to the fixed PPA price of 0.0946 $\frac{€}{\text{kWh}}$. This explains why no optimization is possible and the baseline is the optimal system.

4.2.3 Optimal system combined site

The wood drying kiln's operation is constant throughout the year, apart from the months of March and June where it almost doesn't operate. This becomes evident when consulting Figure 36. These are the times when the SHP does not supply and hence leads to a energy deficit as shown in Figure 37. While the SHP contributes almost 20 %, the Vestas V52 supplies the largest share with 74.8 % of generation. Despite the grid injection limit of 120 kW, a positive grid cash-flow of $\approx 50,000$ € is reached with the grid injection being 45 % larger than the electricity purchase from the grid. Additionally, the SSR of 94 % and SCR of 84 % prove the system to be well balanced. This explains why no optimization is possible for the combined system.

4.2.4 Optimal system combined site SSR

Compared to the baseline, or optimal scenario for NPV optimization, the SSR is improved by 5 % to 99 %. However, this comes at a high price with $1,778,637$ € investment cost and still does not reach 100 % — enabling an off-grid operation of the system. The BG hourly generation profile in Figure 41 shows how its generation supports the system especially during the periods when the SHP generation is low or even zero, for example in March and June. Figure 43 shows a reduction in dried wood available whenever the BG is operating due to its consumption of dried wood chips. Annually, 61 % of the dried wood is directly used in the BG. This leads to a reduction in sold dried wood of 60 % compared with the baseline. The same operating remarks from the BG are also true for the BESS which only shows a higher degree of operation during March while it remains mostly fully charged for the rest of the year as shown in Figure 42. This leads to 18 full charge/discharge cycles per year which is only 5 % of the 365 annual cycles assumed for the cycle life of the BESS. The LCOE_{BG} is much higher than that of the PV system due to its low operating hours throughout the year.

Compared to the baseline, it is possible to reduce the amount of electricity purchased from the grid by 87 % while the electricity sales increased by 25 %. Both can be traced back to the additional generation by PV and the BG. This also shows its effect on the grid cash-flow with an increase of 60 % compared to the baseline. On the other hand, the grid injection limit has a larger impact, increasing the monetary loss per year by 86 % due to the higher generation. The emissions on the other hand decreased by 77 % compared to the baseline. While some of the grid electricity is substituted by the PV system, a bigger fraction of 8.4 % is replaced by the BG which has lower emissions than the grid but does not reduce them to zero like the PV system.

4.2.5 Site comparison

The main comparison of interest is the one from having $P_{optimal}$ and $S_{optimal}$ separately to $C_{optimal}$. With an SCR of 84 % the combined site reaches almost the same value as the primary site while achieving the highest SSR between the scenarios of 94 %. By combining the two separate site into one, the grid cash-flow is reduced by 8.5 % which is caused by a decrease of 11 % in terms of electricity purchased from the grid and a decrease of 35 % of electricity sold to the grid. The latter of which can be traced back to the grid injection limit which is present only in the case of the primary site and the combined site, leading to an increase in monetary loss of 57 % from the combined system to the two separate ones. Generally, more of the consumption of the SHP and Vestas V52 directly supplies the fixed loads. This leads to a reduction of 11 % in dried wood being available to be sold. The biggest improvement is made in terms of emission reductions where the combined system excels with 21.5 % lower emissions per year. The implications of a combined system highlight its better performance in terms of emissions and reduced grid reliance while the single sites show an advantage in terms of grid cash-flow.

5 Conclusion

5.1 Comparison with HOMER Pro

As discussed in subsection 2.5, the results of both models in terms of the real system must be taken with the limitations in mind. Hence, the goal of this comparison is to compare the two models to each other, not to assess whether one scenario or the application of a certain technology is better in the real system then the other. The latter is the focus of the second part of this project. However, from the thorough comparison several major lessons can be derived. Taking into account the comparisons for all scenarios, a general pattern becomes clear. For those scenarios that are grid connected and the same input data in terms of electricity supply and demand are used, both models deliver very similar results. For the primary site, the difference in grid feed-in, electricity purchased from the grid and resulting cash flow difference between the two models is never above 5 %, 35.8 % and 36.4 %, respectively. When the simulation includes a BESS, the more detailed approach used in HOMER Pro delivers more accurate results. However, the difference is small. It even helps to buffer some of the stronger deviations from the grid-tied scenarios. The primary and secondary site show differences for the annual electricity consumed by the loads in the BESS scenarios below 4 % and 15 %, respectively. It is important to note that this can not be considered an improved performance of the HY4RES model in the BESS scenrio but rather a coincidence. Hence, the battery simulation in HY4RES is refined and upgraded for the second part of this project. Remaining differences in simulation results of the two models originate mainly from deviations in input data or the usage of constant hourly data instead of variable ones. It can be expected that with the same input data and modeling, both models would give similar results, as long as no BESS is included. Especially, as the compared values mainly originate from a basic energy balance calculation. As with many other cases does the quality of the input data determine the quality of the results. Thus it is recommended to ensure high quality data that is accurate and represents the real system as close as possible. Additionally, it is advisable to conduct a sensitivity analysis for the uncertain input parameters. Finally, this comparison between the HY4RES model and HOMER Pro can be concluded as a success and the former's simulation capabilities in standard grid-tied scenarios confirmed.

5.2 HY4RES V2

The optimization of the primary site by the Evolutionary method in Excel's Solver, leads to an NPV of 957.85 € and a PP of 23.22 years at a PV installed power of 8 kW. The system does not have a BESS or BG. While the PP is much higher than the average for similar sized installations, the LCOE$_{\text{PV}}$ of 228.3 $\frac{€}{\text{MWh}}$ is within the accepted range. Due to the low NPV the system has an MIRR similar to the discount rate close to 6 %. A sensitivity analysis is carried out on the discount rate, PV investment cost, electricity purchase price and feed-in tariff with a ±10 % change for each. The only negative NPV of −396 € resulted from an increase of the investment cost. Also, a 10 % decrease in feed-in tariff results in a 82 % reduction in NPV to 168 €. The remaining sensitivities lead to positive NPVs. In the best case scenario, a 10 % decrease in investment cost can lead to NPV = 2, 312 €. Even though an optimization and hence expansion of the hybrid energy system is recommended for the primary site, its low NPV means the results should be considered with care. It is recommended to conduct a Monte Carlo simulation on the uncertain parameters and confirm the input parameters with the commercial entity running the site, to compute the probability of the NPV being positive. This can then lead to a more robust recommendation to the operator.

The secondary site and combined site both did not enable an optimization in terms of NPV and hence, the baseline is considered as the optimal scenario. Overall, it can be said that the integration of the wood drying kiln at the primary site in 2024 was an excellent addition to balance the system and make it more viable. To assess the benefits of a combined site which is grid independent, the combined site is maximized for the SSR. With an investment of 1, 778, 637 € and an NPV of −4, 562, 928 €, the combined system SSR reaches 99 %. The optimal configeration being $P_{\text{PV}} = 101$ kW, $P_{\text{BG}} = 247$ kW and $C_{\text{BESS}} = 109$ kWh. While this system leads to a emission reduction of 77 % due to its high SSR, the monetary losses due to the grid injection limit increase by 86 % compared to the combined site baseline. For the operation of the BG, 61 % of the wood dried on site or 408 t are consumed. The BESS only operates when the SHP and BG generation is low, like in the month of March. This leads to 18 full charge/discharge cycles per year, corresponding only to 5 % of the annual cycles recommended by the manufacturer.

One of the main interests of this optimization and simulation is the comparison of two separate sites to one combined site. The combined site reaches an SSR of 94 % and an SCR of 84 %, improving on the SSR of the primary site of 92 % and on the SCR of 64 % of the secondary site. By an reduction of 35 % of electricity feed-in, the monetary losses increase for the combined system by 57 %. Emission reduction on the other hand is reduced by 21.5 %. Hence, it can be said that the combined system outperforms the separate systems in terms of grid independence and carbon emissions while the separate systems perform better on economical aspects. This is true under the assumption that the combined system also adapts the grid injection limit of 120 kW.

Future work should be dedicated to search for alternative paths to circumvent the grid injection limit for the combined site, improving its economic viability. Additionally, a Monte Carlo simulation should be conducted for the optimal primary site to ensure the result's robustness against changes in input parameters. Finally, a more holistic modeling of the site, integrating thermal loads, should be made and the integration of a biomass CHP unit analyzed.

List of Figures

List of Tables

References

1. Schermeyer, H., Vergara, C. & Fichtner, W. Renewable energy curtailment: A case study on today's and tomorrow's congestion management. *Energy Policy* **112,** 427–436. ISSN: 0301-4215 (Jan. 2018).
2. Wind Europe. *EU Grid Action Plan will help renewables, but urgent action needed on excessive connection queues* Online. `https://windeurope.org/newsroom/press-releases/eu-grid-action-plan-will-help-renewables-but-urgent-action-needed-on-excessive-connection-queues/#`, accessed on 10.06.2025. Apr. 2024.
3. Das, K. *et al.* Research Challenges and Opportunities of Utility-Scale Hybrid Power Plants. *WIREs Energy and Environment* **14.** ISSN: 2041-840X (Feb. 2025).
4. Dincer, I., Cozzani, V. & Crivellari, A. in *Hybrid Energy Systems for Offshore Applications* 7–18 (Elsevier, 2021). ISBN: 9780323898232.
5. Ahmad Khan, A. *et al.* Optimal Sizing, Techno-Economic Feasibility and Reliability Analysis of Hybrid Renewable Energy System: A Systematic Review of Energy Storage Systems' Integration. *IEEE Access* **13,** 59198–59226. ISSN: 2169-3536 (2025).
6. Coelho, J. S. T. *et al.* Multi-Objective and Multi-Variable Optimization Models of Hybrid Renewable Energy Solutions for Water–Energy Nexus. *Water* **16,** 2360. ISSN: 2073-4441 (Aug. 2024).
7. Coelho, J. *et al.* Hybrid Energy Solution to Improve Irrigation Systems: HY4RES vs. HOMER Optimization Models. *Energies* **17,** 4037. ISSN: 1996-1073 (Aug. 2024).
8. Ramos, H. M. *et al.* Optimization and Machine Learning in Modeling Approaches to Hybrid Energy Balance to Improve Ports' Efficiency. *Applied Sciences* **15,** 5211. ISSN: 2076-3417 (May 2025).
9. Ramos, H. M., Pina, J., Coronado-Hernández, O. E., Pérez-Sánchez, M. & McNabola, A. Conceptual hybrid energy model for different power potential scales: Technical and economic approaches. *Renewable Energy* **237,** 121486. ISSN: 0960-1481 (Dec. 2024).
10. Interreg Atlantic Area HY4RES. *Aquaculture pilot site Ireland* Online. `https://hy4res.eu/pilot-sites/aquaculture/`, accessed on 11.04.2025.
11. Thirunavukkarasu, M., Sawle, Y. & Lala, H. A comprehensive review on optimization of hybrid renewable energy systems using various optimization techniques. *Renewable and Sustainable Energy Reviews* **176,** 113192. ISSN: 1364-0321 (Apr. 2023).
12. Gusain, C., Nangia, U. & Tripathi, M. M. Optimal sizing of standalone hybrid renewable energy system based on reliability indicator: A case study. *Energy Conversion and Management* **310,** 118490. ISSN: 0196-8904 (June 2024).
13. Ukoima, K. N., Okoro, O. I., Obi, P. I., Akuru, U. B. & Davidson, I. E. Optimal Sizing, Energy Balance, Load Management and Performance Analysis of a Hybrid Renewable Energy System. *Energies* **17,** 5275. ISSN: 1996-1073 (Oct. 2024).
14. Bekci, E. *HY4RES Project - Aquaculture in Ireland HOMER Pro simulation report*
15. Sari, E., Güven, Y. & Aktaş, M. Güneş Enerjili Eko Tasarım Kereste Kurutma Sistemi. *Politeknik Dergisi* **27,** 1473–1489. ISSN: 2147-9429 (Sept. 2024).

16. Pfenninger, S. & Staffell, I. Long-term patterns of European PV output using 30 years of validated hourly reanalysis and satellite data. *Energy* **114,** 1251–1265. ISSN: 0360-5442 (Nov. 2016).

17. wind-turbine-models.com. *Vestas V52* Online. https://en.wind-turbine-models.com/turbines/71-vestas-v52, accessed on 29.04.2025. June 2023.

18. European Comission Joint Research Centre Energy Efficiency and Renewables Unit. *Photovoltaic Geographical Information System (PVGIS)* Online. https://re.jrc.ec.europa.eu/pvg_tools/en/, accessed on 10.06.2025. Dec. 2024.

19. Bates, J. & Howes, P. *Potential Biomass Prices in Ireland* tech. rep. (Ricardo Energy & Environment, 2017).

20. O'Brien Timber Products Ltd. *Frequently Asked Questions* Online. https://www.celticlogs.ie/faq.php, accessed on 06.05.2025.

21. Energy Research Centre of the Netherlands (ECN). *Phyllis, Data Base for Biomass and Waste* Online. https://phyllis.nl/Browse/Standard/ECN-Phyllis#sitka, accessed on 06.05.2025. 2009.

22. Gonzalez, A., Riba, J.-R., Puig, R. & Navarro, P. Review of micro- and small-scale technologies to produce electricity and heat from Mediterranean forests' wood chips. *Renewable and Sustainable Energy Reviews* **43,** 143–155. ISSN: 1364-0321 (Mar. 2015).

23. Ahrenfeldt, J. *et al.* Validation of a Continuous Combined Heat and Power (CHP) Operation of a Two-Stage Biomass Gasifier. *Energy & Fuels* **20,** 2672–2680. ISSN: 1520-5029 (Oct. 2006).

24. Gonzalez, A., Riba, J.-R., Esteban, B. & Rius, A. Environmental and cost optimal design of a biomass–Wind–PV electricity generation system. *Renewable Energy* **126,** 420–430. ISSN: 0960-1481 (Oct. 2018).

25. NREL. *Annual Technology Baseline Commercial Battery Storage* Online. https://atb.nrel.gov/electricity/2024/commercial_battery_storage, accessed on 24.05.2025.

26. Irish Tax and Customs. *Corporation Tax (CT)* Online. https://www.revenue.ie/en/companies-and-charities/corporation-tax-for-companies/corporation-tax/basis-of-charge.aspx, accessed on 09.05.2025.

27. Indrawan, N., Simkins, B., Kumar, A. & Huhnke, R. L. Economics of Distributed Power Generation via Gasification of Biomass and Municipal Solid Waste. *Energies* **13,** 3703. ISSN: 1996-1073 (July 2020).

28. Environmental Protection Agency. *ETS2 (buildings, road transport and additional sectors (other small industry))* Online. https://www.epa.ie/our-services/licensing/climate-change/eu-emissions-trading-system-/eu-emissions-trading-system-2-ets2/#d.en.128248, accessed on 12.05.2025. 2025.

29. Irish Tax and Customs. *Solid Fuel Carbon Tax (SFCT)* Online. https://www.revenue.ie/en/companies-and-charities/excise-and-licences/energy-taxes/solid-fuel-carbon-tax/reliefs.aspx, accessed on 12.05.2025. May 2025.

30. JA Solar. *JAM60D42 LB* Online. https://www.jasolar.eu/en/products/jam60d42-lb, accessed on 23.05.2025.

31. Abbes, D., Martinez, A. & Champenois, G. Life cycle cost, embodied energy and loss of power supply probability for the optimal design of hybrid power systems. *Mathematics and Computers in Simulation* **98,** 46–62. ISSN: 0378-4754 (Apr. 2014).

32. Colantoni, A. *et al.* Economic analysis and risk assessment of biomass gasification CHP systems of different sizes through Monte Carlo simulation. *Energy Reports* **7,** 1954–1961. ISSN: 2352-4847 (Nov. 2021).

33. Correia, D. M. Q. *Technoeconomic analysis of a trigeneration system based on biomass gasification* PhD thesis (Mechanical Engineering, 2017).

34. Dufo-Lopez, R., Bernal-Agustin, J. L. & Mendoza, F. Design and economical analysis of hybrid PV–wind systems connected to the grid for the intermittent production of hydrogen. *Energy Policy* **37,** 3082–3095. ISSN: 0301-4215 (Aug. 2009).

35. Martin, L. *What is the Cost of Commercial Solar Panels in Ireland?* Online. `https://spvenergy.ie/commercial-solar-panels-cost-ireland/`, accessed on 23.05.2025.

36. IRENA. *RENEWABLE ENERGY TECHNOLOGIES: COST ANALYSIS SERIES - Biomass for Power Generation* tech. rep. (IRENA, 2012).

37. U.S. Environmental Protection Agency. *Biomass Combined Heat and Power Catalog of Technologies* tech. rep. (U.S. Environmental Protection Agency, 2015).

38. SEAI. *Non-domestic microgen grant* Online. `https://www.seai.ie/grants/business-grants/commercial-solar-pv`, accessed on 26.05.2025.

39. Bates, J., Matthews, R. & Mortimer, N. *Including UK and international forestry in Biomass Environmental Assessment Tool (BEAT2)* tech. rep. (Environment Agency, 2011).

40. Currents by Green Collective. *Irish Grid Monthly Recap, February 2025* Online. `https://currents.greencollective.io/irish-grid-monthly-recap-february-2025/`, accessed on 12.05.2025. Mar. 2025.

41. seai. *Solar electricity calculator* Online. `https://www.seai.ie/about/tools/solar-electricity-calculator`, accessed on 17.06.2025.

42. Lazard. *Levelized Cost of Energy+* tech. rep. (Lazard, June 2024).